# Temperature-dependent electronic structure and magnetic behavior of Mott insulators

W. Nolting,* L. Haunert, and G. Borstel
*Fachbereich Physik, Universität Osnabrück, Barbarastrasse 7, D-4500 Osnabrück, Germany*
(Received 26 December 1990; revised manuscript received 1 October 1991)

We investigate the temperature-dependent electronic and magnetic properties of transition-metal monoxides by use of a theoretical model that takes into account the $3d$ subbands of the transition metal and the oxygen $2p$ subbands. Characteristic properties of these Mott insulators are caused by strong $3d$-electron correlations, described by intra-atomic Coulomb interactions and characterized by three different coupling constants: $U$, $\bar{U}$, and $J$. The intraband coupling $U$ turns out to be decisive for the appearance of spontaneous antiferromagnetism. $\bar{U}$ is a direct interband Coulomb interaction responsible for a nonuniform occupation of the $3d$ subbands, and therewith decisive for the insulator properties of these materials. The interband exchange $J$ describes an effective electron-magnon interaction and polarizes magnetically inactive subbands. The self-consistent solution of our model yields a quasiparticle density of states that contains three nonconnected energy regions with predominantly $3d$ character: two below, and one above, the chemical potential $\mu$. The insulator gap is practically temperature independent, persisting for arbitrary $T \gg T_N$. A necessary condition for the insulating behavior is an integral number $n_{3d} \geq 5$ of $3d$ electrons. The antiferromagnetism is caused by $10-n_{3d}$ exactly half-filled $3d$ subbands, while $n_{3d}-5$ subbands are completely filled. The magnetic moment remains stable for arbitrarily high temperatures. The temperature dependence of the sublattice magnetization is caused by a "kinetic Heisenberg exchange." The $2p$-$3d$ hybridization plays only a minor role with respect to the magnetic and insulating properties of Mott insulators, but becomes decisive for the nature of the band gap and the interpretation of photoemission data. Our model calculation correctly predicts MnO, FeO, CoO, NiO, and CuO to be antiferromagnetic insulators, while VO turns out to be a nonmagnetic metal.

## I. INTRODUCTION

The electronic structure and the magnetic properties of $3d$-metal monoxides (NiO, CoO, FeO, MnO) have been the target of immense research activities for about 50 years,[1] and simultaneously the subject of rather controversial discussions. They are commonly called "Mott insulators," although there is obviously up to now no general agreement upon how to define this term. Are they simply to be identified with ordinary "magnetic insulators," as put forward by Brandow,[2,3] or do they represent a completely different class of insulators?

Normal magnetic insulators (EuO, EuTe, $CrBr_3$, $GdCl_3$, $K_2CuF_4$, ...) are well described by the Heisenberg model as far as their purely magnetic properties are concerned. This model presumes strictly localized magnetic moments, as realized, e.g., by partially filled $4f$ shells in certain rare-earth compounds. According to photoemission experiments, there is, however, little evidence that the $3d$ electrons in transition-metal monoxides are strictly localized. But insulation does not necessarily mean localization. It may also be caused by the existence of excludingly filled or empty energy bands. On the other hand, in such a case conventional band theory cannot justify the appearance of permanent magnetic moments. Nevertheless, prototypical Mott insulators like NiO evidently take their permanent moment from completely filled subbands with dispersions as large as some 2 eV.[4,5] This is explainable only if correlation effects account for a splitting of the Bloch band into several quasiparticle subbands, which may produce a nonzero moment even if they are completely filled.

Some authors discuss the insulating state of Mott materials without any reference to (antiferro)magnetism. In our opinion this is not sufficient. A convincing model for Mott insulators must also explain the simultaneous existence of an insulator gap and a magnetic moment, both persisting for temperatures $T \gg T_N$. Conventional band calculations,[6,7] which implicitly use Slater's theory of antiferromagnetism, put the Fermi edge into the so-called Slater gap, caused by the antiferromagnetic structure which halves the Brillouin zone of the chemical lattice, therewith predicting, for $T=0$, MnO and NiO as antiferromagnetic narrow gap semiconductors. Such an explanation of the Mott insulation implies, contrary to experiment, that MnO and NiO would become metals above $T_N$. Applied to FeO and CoO, this model fails, even for arbitrarily low temperatures, to predict the insulating state.

Although such a reference of Mott insulation to antiferromagnetism does not work, there is another link between electronic and magnetic properties of these materials. De Boer and Verwey[1] point out that the insulating behavior of transition-metal oxides like NiO, CoO, MnO, $Fe_2O_3$, $Mn_2O_3$, ... is necessarily bound to an integral number of $3d$ electrons per cation. Small deviations from stoichiometry make these oxides metallic. $Fe_3O_4 = FeO \cdot Fe_2O_3$ is metallic, although FeO as well as $Fe_2O_3$ are insulators. The reason is the valence mixing ($Fe^{2+}$,$Fe^{3+}$) which leads to a nonintegral number of elec-

 

trons $n_{3d}$ per cation. On the other hand, if $n_{3d}$ is an integer ( $<10$), then there is a chance that one or more of the five $3d$ subbands is just half-filled, a situation which favors antiferromagnetism in highly correlated electron systems.[8-10]

Combined photoemission and inverse-photoemission spectroscopy[4,11] for NiO has revealed that there exist three energy regions in which $3d$ states appear. One part lies some 9 eV below the chemical potential $\mu$. The second part overlaps with the oxygen $2p$ subbands, therewith strongly hybridizing with them. The third $3d$ energy region can be detected by inverse photoemission, being some 4 eV above the occupied part of the spectrum,[5,12] which agrees with the optically determined NiO gap.[13] The important point is that the insulator gap is stable for arbitrary temperatures $T \gg T_N$. The nature of this insulator gap has attracted intensive research work in the past. Fujimori, Minami, and Sugano[14,15] performed local-cluster calculations (e.g., $Ni^{2+}$ ions octahedrally coordinated by closed-shell $O^{2-}$ ions), within the configuration-interaction (CI) formalism, and compared their results to x-ray photoemission spectroscopy (XPS) experiments.[16] They found that, at threshold, the final state should be predominantly due to a $3d$ hole which is strongly screened by a ligand-to-$3d$ charge transfer. In the language of spectroscopy, this final state is mainly of $3d^8L^{-1}$ character, where $L^{-1}$ stands for a ligand hole. On the other hand, the lowest excited electron state is undoubtedly of $3d^9$ type. NiO is therefore called a charge-transfer insulator.[5,14,15] This picture has been taken up and confirmed by other authors.[17,18] The low-energy $3d$ part near 9 eV of the photoemission spectrum is explained by $d^7$ final states.[4,14,15] Small-cluster calculations like those of Fujimori, Minami, and Sugano[14,15] or the more recent *ab initio* calculations of Janssen and Nieuwpoort[19] have the advantage of offering full insight into multiplet structures of the various transitions. The connection of the electronic structure to the insulator problem and antiferromagnetism is, however, largely suppressed.

As already mentioned, conventional band calculations, performed within the local-spin-density approximation (LSDA) fail to describe in a physically correct manner the insulator properties of the transition-metal monoxides, but they can reproduce rather well the antiferromagnetic structure of these materials.[7] In order to judge the merits of band calculations based on density-functional theory (DFT) for such systems, one must bear in mind that DFT is strictly a ground-state theory in which only the ground-state energy $E_0(N)$ of the $N$-electron system and the corresponding spin densities have physical importance. In particular, the one-electron eigenvalues and wave functions of DFT have, in general, no strict physical meaning at all. Thus, DFT, in principle, should be able to describe the antiferromagnetism and the insulating ground state of Mott insulators at $T=0$, where the band gap of an $N$-electron system is rigorously given in terms of ground-state energies by

$$E_G = E_0(N+1) + E_0(N-1) - 2E_0(N) \ .$$

In a strict sense, however, DFT provides no information on the orbital character of the gap or the spectrum of other excitations in these systems. Within these limitations of DFT, the recent proposals for an *ab initio* type description of Mott insulators at $T=0$ in a "self-interaction corrected"[20] (SIC) or "unoccupied-states potential corrected"[21,22] (USPC) formulation of density-functional theory represent interesting theoretical developments. They may complement our present work.

Let us now summarize some of the most important questions and problems provoked by the above-discussed phenomena of Mott insulators: (1) Why do the $3d$ transition-metal monoxides represent insulators in contrast to elementary band theory? (2) Why are they antiferromagnets? (3) What kind of theoretical model is appropriate? (4) What is the physical reason for the appearance of three nonconnected $3d$ quasiparticle energy regions? (5) Why is obviously the integral number of $3d$ electrons per cation a necessary condition for the insulating behavior of transition-metal oxides? (6) How does antiferromagnetism manifest itself in an electronic band structure? Is there any possibility to get the characteristic magnetic data like the Néel temperature $T_N$, the magnetic $T=0$ moment, etc., as self-consistent solutions of a proper theoretical model? (7) What is the reason for the remarkable failure of standard high-quality band-structure calculations? (8) Can a Mott insulator be ferromagnetic? (9) What is the reference to "normal" Heisenberg antiferromagnets? (10) How do the prototypes NiO, CoO, FeO, MnO differ from one another? Is there any systematic trend in the physical data? (11) What is the role of the $3d$-$2p$ hybridization? (12) Is the insulator gap of $3d$-$3d$ or of $2p$-$3d$ character? (13) Is there any systematic when going from NiO to NiS? It is the aim of this paper to demonstrate by use of a properly defined theoretical model that all these problems and questions find a natural explanation as direct consequences of strong electron correlations.

In previous studies we have investigated the Heisenberg ferromagnet EuO (Ref. 23) and the band ferromagnet Ni (Refs. 24 and 25) by use of a technique which we called a "renormalized" many-body procedure. The main goal was to derive a theory which permits a quantitative comparison to the experiment. For this purpose we first constructed a proper theoretical model. In the one-particle part of the model Hamiltonian, we then implemented the results of a full self-consistent band-structure calculation. In the final step we applied to the total Hamiltonian a reliable many-body procedure in order to get information about the temperature dependence of fundamental quasiparticle quantities like self-energy, spectral density, and quasiparticle density of states. A similar approach is intended here for the Mott insulators. In such a procedure the most important step is to find a reasonable model. The main part of our proposal, which we present in the next sections, is the intra-atomic Coulomb interaction between the Ni $3d$ electrons, while the oxygen $2p$ bands turn out to be not decisive for the magnetic and insulating properties of typical Mott insulators like the transition-metal monoxides. We shall show that the Ni $3d$ Coulomb correlations may be divided into three characteristic portions, one intraband and two in-

terband contributions. The intraband term has exactly the operator structure of the Hubbard model[26] with a coupling constant $U$ of some 12 eV. It is the most decisive part that concerns the origin of the spontaneous antiferromagnetism.[8,9] One of the two interband terms has the structure of the well-known $s$-$f$ model[23] with an exchange constant $J$ of some tenth of an eV, and may be interpreted as an effective electron-magnon scattering. The other interband interaction looks like a normal Coulomb interaction between charge densities, which belong to different subbands. The respective coupling constant $\bar{U}$ is of the same order of magnitude as the intraband constant $U$. We shall show that a certain interplay between $U$ and $\bar{U}$ explains the Mott insulation and the antiferromagnetism in systems like NiO, CoO, FeO, and MnO.

In Sec. II, we present a detailed discussion of the theoretical model which we shall apply to the antiferromagnetic transition-metal monoxides. Section III is then devoted to our rather sophisticated many-body approach, the results of which are discussed in Sec. IV.

## II. THEORETICAL MODEL

### A. General formalism

The four transition-metal monoxides NiO, CoO, FeO, and MnO all crystallize in the rocksalt structure, i.e., the metal ions and the oxygen ions, respectively, occupy lattice sites of a fcc structure. In order to be able to describe simultaneously antiferromagnetism as well as paramagnetism and ferromagnetism, we further decompose the fcc structure into two chemically equivalent sublattices $A$ and $B$. The (111) planes shall belong in alternating sequence to $A$ and $B$, respectively. We refer to the total (Ni, Co, Fe, Mn) lattice or to the O lattice as a Bravais lattice ($\mathbf{R}_i$) with a two-atom basis ($\mathbf{r}_\alpha$). The space vector of any lattice site is then given by

$$\mathbf{R}_{i\alpha}=\mathbf{R}_i+\mathbf{r}_\alpha \quad (i=1,2,\ldots,N,\ \alpha=A,B)\ , \tag{2.1}$$

$N$ is the number of sites in the Bravais lattice, $2N$ in the cation (anion) fcc lattice, and $4N$ in the full rocksalt structure. The thermodynamic average of any site-dependent operator $O_{i\alpha}$,

$$\langle O_{i\alpha}\rangle=\langle O_\alpha\rangle \tag{2.2}$$

is $\mathbf{R}_i$ independent but may depend on the sublattice index $\alpha$, as far as antiferromagnetic phases are considered. Fourier transformations between real space and $\mathbf{k}$ space are restricted to the Bravais lattice and its corresponding Brillouin zone:

$$O_{i\alpha}=N^{-1/2}\sum_{\mathbf{k}}\exp(i\mathbf{k}\cdot\mathbf{R}_i)O_{\mathbf{k}\alpha}\ , \tag{2.3}$$

$$O_{\mathbf{k}\alpha}=N^{-1/2}\sum_{i}\exp(-i\mathbf{k}\cdot\mathbf{R}_i)O_{i\alpha}\ . \tag{2.4}$$

### B. Model

For a proper description of the electronic and magnetic data of the prototypical Mott insulators NiO, CoO, FeO, and MnO we need a model which contains as essential ingredients the cation $3d$ and the oxygen $2p$ subbands:

$$H=H_{3d}+H_{3d\text{-}3d}+H_{2p}+H_{3d\text{-}2p}\ . \tag{2.5}$$

The spontaneous antiferromagnetism originates excludingly from the $3d$ bands of the transition metal. $H_{3d\text{-}3d}$ is therefore the most important part of the model Hamiltonian. The O $2p$ subbands are magnetically inactive. Nevertheless, they cannot be neglected because they influence the relevant $3d$ bands by a more or less strong hybridization $H_{3d\text{-}2p}$.

The one-particle operator $H_{3d}$ describes the kinetic energy of the $3d$ electrons and their interaction with the periodic lattice potential:

$$H_{3d}=\sum_{\substack{i,j,\sigma,\\ \alpha,\beta,m}} T_{ij}^{\alpha\beta}(m)c_{i\alpha m\sigma}^{\dagger}c_{j\beta m\sigma}\ . \tag{2.6}$$

$c_{i\alpha m\sigma}^{\dagger}$ ($c_{i\alpha m\sigma}$) is the creation (annihilation) operator of a $3d$ electron with spin $\sigma$ at site $\mathbf{R}_{i\alpha}$ in the $m$th subband ($m=1,2,\ldots,5$). $T_{ij}^{\alpha\beta}(m)$ is the hopping integral between $\mathbf{R}_{i\alpha}$ and $\mathbf{R}_{j\beta}$, being related to the $\mathbf{k}$-dependent Bloch energies by

$$\varepsilon_m^{\alpha\beta}(\mathbf{k})=(1/N)\sum_{i,j}T_{ij}^{\alpha\beta}(m)\exp[-i\mathbf{k}\cdot(\mathbf{R}_i-\mathbf{R}_j)]\ . \tag{2.7}$$

In a tight-binding approximation we restrict the electron hopping to nearest [$T_1(m)$] and next-nearest neighbors [$T_2(m)$] in the chemical lattice. The resulting Bloch density of states $\rho_{0m}(E)$ (B-DOS) of the noninteracting electrons in the $m$th subband (Fig. 1) is then determined by three parameters, the center of gravity $T_0(m)$, the bandwidth $W_m$, and the ratio $T_2(m)/T_1(m)$. Details of the explicit derivation of the B-DOS are presented in Appendix A. It should be emphasized, however, that the tight-binding approximation is not a necessary ingredient of our theory. In fact, the Bloch energies (2.7) could also have been taken from more realistic band-structure calculations as, e.g., exemplified in Ref. 23 for EuO.

The striking phenomena of the transition-metal

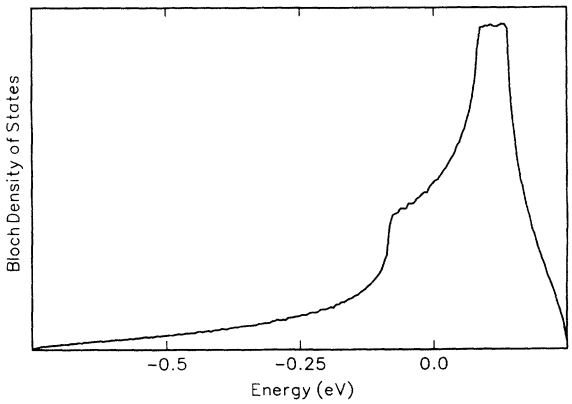


FIG. 1. Tight-binding version of the Bloch density of states $\rho_{0m}$ for a fcc lattice, including nearest and next-nearest hopping, as function of energy. Bandwidth $W=1$ eV, center of gravity $T_0(m)=0$ eV.

monoxides may be traced back rather excludingly to strong electron correlations within the $3d$ subbands of the transition metal. We refer to them by the Hamiltonian $H_{3d\text{-}3d}$ in (2.5). This operator represents the electron-electron Coulomb interaction which we consider as so strongly screened that only intra-atomic contributions will be of importance. To keep the model Hamiltonian as simple as possible, but without losing the essential ingredients for band magnetism, we restrict the Coulomb matrix elements to so-called direct ($U_{mm'}$) and exchange terms ($J_{mm'}$):

$$H_{3d\text{-}3d}=\tfrac{1}{2}\sum_{\substack{i,\alpha,\sigma,\sigma'\\ m,m'}}[\,U_{mm'}c^{\dagger}_{i\alpha m\sigma}c^{\dagger}_{i\alpha m'\sigma'}c_{i\alpha m'\sigma'}c_{i\alpha m\sigma}+J_{mm'}c^{\dagger}_{i\alpha m\sigma}c^{\dagger}_{i\alpha m'\sigma'}c_{i\alpha m\sigma'}c_{i\alpha m'\sigma}\,] \quad (2.8)$$

Because of its decisive importance, we present a further detailed inspection of the operator $H_{3d\text{-}3d}$ in the next section.

The $2p$ energy bands of the oxygen are fully occupied. We thus can restrict the influence of the respective electron-electron interaction simply to a proper renormalization of the one-particle energies:

$$H_{2p}=\sum_{\substack{i,j,\sigma,\\ \alpha,\beta,\mu}}T^{\alpha\beta}_{ij}(\mu)b^{\dagger}_{i\alpha\mu\sigma}b_{j\beta\mu\sigma}\ . \quad (2.9)$$

The corresponding Bloch energies $\varepsilon^{\alpha\beta}_{\mu}(\mathbf{k})$ are defined in strict analogy to those in (2.7) of the $3d$ bands. The cation and anion lattices are completely identical, only rigidly shifted against one another by one-half the lattice constant. This manifests itself in an unimportant phase factor for the hopping integrals, so that we may formally consider the $2p$ electrons moving in the same fcc lattice as the $3d$ electrons. $b^{\dagger}_{i\alpha\mu\sigma}$ ($b_{i\alpha\mu\sigma}$) is the creation (annihilation) operator of a $2p$ electron with spin $\sigma$ at site $\mathbf{R}_{i\alpha}$ in the subband with index $\mu$ ($\mu=1,2,3$).

$H_{3d\text{-}2p}$ expresses the hybridization between Ni $3d$ and O $2p$ subbands, for which we use the $\mathbf{k}$ representation

$$H_{3d\text{-}2p}=\sum_{\mu,m}\sum_{\substack{\mathbf{k},\sigma,\\ \alpha,\beta}}[\,V^{\alpha\beta}_{\mathbf{k}\mu m}b^{\dagger}_{\mathbf{k}\alpha\mu\sigma}c_{\mathbf{k}\beta m\sigma}+(V^{\alpha\beta}_{\mathbf{k}\mu m})^{*}c^{\dagger}_{\mathbf{k}\beta m\sigma}b_{\mathbf{k}\alpha\mu\sigma}\,] \quad (2.10)$$

We consider the Ni $3d$ bands and the O $2p$ bands, respectively, as completely equivalent with respect to the hybridization, so that the $\mu,m$ dependence of $V$ will be neglected. If necessary, this simplification may easily be removed. Hybridization effects between different $3d$ subbands or between different $2p$ subbands are thought to be sufficiently accounted for by a proper renormalization of the one-particle energies.

### C. Transition-metal-electron correlations

Let us now inspect in detail the interaction part $H_{3d\text{-}3d}$ which is responsible for the decisive electron correlations in the $3d$ subbands. Introducing the spin-independent occupation number operator,

$$\hat{n}_{i\alpha m}=\sum_{\sigma}c^{\dagger}_{i\alpha m\sigma}c_{i\alpha m\sigma}=\sum_{\sigma}n_{i\alpha m\sigma}\ , \quad (2.11)$$

the interaction term (2.8) may be rearranged as follows:

$$H_{3d\text{-}3d}=\tfrac{1}{2}\sum_{\substack{i,m,m',\alpha\\ (m\neq m')}}(U_{mm'}-\tfrac{1}{2}J_{mm'})\hat{n}_{i\alpha m}\hat{n}_{i\alpha m'}+\tfrac{1}{2}\sum_{i,\alpha,m,\sigma}(U_{mm}+J_{mm})n_{i\alpha m\sigma}n_{i\alpha m-\sigma}$$
$$-\tfrac{1}{2}\sum_{\substack{i,m,m',\alpha,\sigma\\ (m\neq m')}}J_{mm'}\left[\tfrac{1}{2}\sum_{\sigma'}z_{\sigma}z_{\sigma'}n_{i\alpha m\sigma}n_{i\alpha m\sigma'}+c^{\dagger}_{i\alpha m\sigma}c_{i\alpha m-\sigma}c^{\dagger}_{i\alpha m'-\sigma}c_{i\alpha m'\sigma}\right]\ . \quad (2.12)$$

$n_{i\alpha m\sigma}=c^{\dagger}_{i\alpha m\sigma}c_{i\alpha m\sigma}$ is the occupation number operator, and $z_{\sigma}$ is a sign factor: $z_{\uparrow}=+1$ and $z_{\downarrow}=-1$. We consider the various $3d$ subbands as completely equivalent, and thus suppress as far as possible the band index dependence of the matrix elements:

$$U=U_{mm}+J_{mm}\ ,$$
$$\bar{U}=U_{mm'}-\tfrac{1}{2}J_{mm'}\ (m\neq m')\ , \quad (2.13)$$
$$J=J_{mm'}\ (m\neq m')\ .$$

Equation (2.12) then implies that the interaction $H_{3d\text{-}3d}$ consists of three characteristic partial operators:

$$H_{3d\text{-}3d}=H^{(U)}_{3d}+H^{(J)}_{3d}+H^{(\bar{U})}_{3d}\ . \quad (2.14)$$

The first operator represents an intraband interaction which has exactly the structure of the multiband Hubbard Hamiltonian:[26]

$$H^{(U)}_{3d}=U\sum_{i,\alpha,m}n_{i\alpha m_{\uparrow}}\cdot n_{i\alpha m_{\downarrow}}\ . \quad (2.15)$$

We recognize that the Hubbard model, frequently used for describing electron correlations in narrow energy bands, is one part of our more generalized model of magnetism. $H^{(U)}_{3d}$ turns out to be of crucial importance for the possibility of spontaneous magnetic order.[24,25] In highly correlated electron systems ($U\gg$Bloch bandwidth), $H^{(U)}_{3d}$ splits each nondegenerate energy band into two quasiparticle subbands separated by an energy amount of order $U$.[8,9,27] This splitting does not change very much with temperature, in particular, it is not bound to any magnetic order. Under certain conditions, mainly on the Coulomb coupling $U$, on the lattice structure, and on the degree of band filling, each of the two quasiparticle subbands splits once more into two spin bands ("exchange splitting") producing therewith spontaneous (anti)ferromagnetism.[8,9,27] Because of its decisive importance, the partial operator $H^{(U)}_{3d}$ is further discussed in the next subsection.

The second term in (2.14) represents an interband exchange interaction. After introducing electron spin operators,

$$\sigma^z_{i\alpha m}=\tfrac{1}{2}\sum_\sigma z_\sigma n_{i\alpha m\sigma}\ ,$$
$$\sigma^+_{i\alpha m}=c^\dagger_{i\alpha m\uparrow}c_{i\alpha m\downarrow}\ , \tag{2.16}$$
$$\sigma^-_{i\alpha m}=c^\dagger_{i\alpha m\downarrow}c_{i\alpha m\uparrow}\ .$$

$H^{(J)}_{3d}$ has exactly the same structure as the interaction term of the well-known $s$-$f$ ($d$-$f$) model[23] which is therefore also one part of our generalized model:

$$H^{(J)}_{3d}=-J\sum_{i,\alpha,m}[\sigma^z_{i\alpha m}S^z_{i\alpha m}+\tfrac{1}{2}(\sigma^+_{i\alpha m}S^-_{i\alpha m}+\sigma^-_{i\alpha m}S^+_{i\alpha m})]\ . \tag{2.17}$$

$\mathbf{S}_{i\alpha m}$ is an effective, localized spin, which interacts at site $\mathbf{R}_{i\alpha}$ with an electron from subband $m$. It is built up by the electron spins of all other subbands $m'\neq m$:

$$S^\eta_{i\alpha m}=\sum_{m'\ (\neq m)}\sigma^\eta_{i\alpha m'},\quad \eta=+,-,z\ . \tag{2.18}$$

The first term in (2.17) represents an Ising-like interaction between electron spin and effective spin, which accounts for more or less rigid band shifts. The second term describes spin-exchange processes of the band electron with the effective, localized spin system, which may result, e.g., in an effective electron-magnon scattering.

The third term $H^{(\bar U)}_{3d}$ in (2.14) represents another interband coupling which may be interpreted as a direct Coulomb interaction between charge densities belonging to different subbands:

$$H^{(\bar U)}_{3d}=\tfrac{1}{2}\bar U\sum_{\substack{i,\alpha,m,m'\\(m\neq m')}}\hat n_{i\alpha m}\hat n_{i\alpha m'}\ . \tag{2.19}$$

The electron from the $m$th subband interacts with the electrons of all the other subbands, but not with those from its own subband. Because of its spin independence, $H^{(\bar U)}_{3d}$ will be rather unimportant for magnetic phenomena. It plays, however, a non-negligible role with respect to the insulator properties of the transition-metal monoxides. As we shall demonstrate, $H^{(\bar U)}_{3d}$ may provoke situations where it is energetically more favorable for the system to distribute its $3d$ electrons nonuniformly over, in principle, equivalent subbands. That leads to different fillings of the $3d$ subbands and therewith to a decisive orbital polarization.[3]

It is worthwhile to stress once more that the basic possibility for the appearance of spontaneous (anti)ferromagnetism is excludingly due to the intraband interaction $H^{(U)}_{3d}$. As soon as spontaneous (anti)ferromagnetism does appear, the interband exchange $H^{(J)}_{3d}$ can, however, strongly modify the magnetic data (transition temperature, $T=0$ moment, ...).[24,25] The third term $H^{(\bar U)}_{3d}$ may have substantial influence on conductivity properties (metal or insulator?), but is unimportant for magnetic features.

### D. Kinetic exchange

In Eq. (2.14), the decisive interaction operator $H_{3d\text{-}3d}$ is decomposed into three partial operators with very clear physical meanings. As to the magnetic properties, the intraband interaction $H^{(U)}_{3d}$ plays a dominant role and must therefore be handled with special care. In the following we try to get further insight into the physics mediated by this term. For this purpose we reformulate $H^{(U)}_{3d}$ by a suitable canonical transformation in order to extract certain terms which will give rise to collective spin excitations. These turn out to be especially important in the case of exactly half-filled bands ($n_m=1$) in the split-band regime ($U\gg W_m$) when normal one-electron excitations become rather unlikely. We follow very closely a previous proposal of Chao, Spalek, and Oleś,[28] which has recently experienced a dramatic upsurge in connection with the so-called $t$-$J$ model[29] for the description of high-$T_c$ superconductors. We modify the procedure in a proper way for our purposes.

The starting point is the following single-band Hamiltonian:

$$H_U(m)=\sum_{i,j,\alpha,\beta,\sigma}T^{\alpha\beta}_{ij}(m)c^\dagger_{i\alpha m\sigma}c_{j\beta m\sigma}+U\sum_{i,\alpha}n_{i\alpha m\uparrow}n_{i\alpha m\downarrow}\ , \tag{2.20}$$

which enters our model via

$$H_{3d}+H^{(U)}_{3d}=\sum_m H_U(m)\ . \tag{2.21}$$

In the zero bandwidth limit ($W_m\to 0$; $W_m$, width of the $m$th subband of the noninteracting electron system), the operator $H_U(m)$ produces two quasiparticle levels at energies $T_0(m)$ and $T_0(m)+U$ with temperature, carrier-concentration, and spin degrees of degeneracy $[1-\langle n_{i\alpha m-\sigma}\rangle]N$ and $\langle n_{i\alpha m-\sigma}\rangle N$, respectively. For the case of finite hopping probabilities, the degenerate levels will be spread to quasiparticle subbands with finite widths, which, however, remain well separated in the strong-coupling regime $U\gg W_m$. The physical meaning of these two quasiparticle subbands can be understood in very simple terms. When an electron jumps excludingly onto sites, which do not contain any other electron of the same subband $m$, then it will never perform an intraband Coulomb interaction $U$, being therefore surely within the lower subband centered around $T_0(m)$. Analogously, an electron, which always chooses places, where it meets another electron with opposite spin, is moving, of course, in the upper quasiparticle subband. These are the unambiguous cases. Not so uniquely to be classified are, however, intersublevel transitions as those schematically plotted in Fig. 2. They are the less likely the larger $U$ and must be interpreted as "virtual transitions." Nevertheless, they may possess, even in the strong-coupling regime, a non-negligible influence on the quasiparticle energy spectrum, as we shall recognize below.

We decompose the operator (2.20) into two parts

$$H_U(m)=H^{(0)}_U(m)+H^{(1)}_U(m)\ . \tag{2.22}$$

$H^{(0)}_U(m)$ shall describe the "pure" quasiparticle propagation in one of the two subbands. It shall contain all those terms which, in the last analysis, may be interpreted at least as an "effective" hopping in the lower or upper

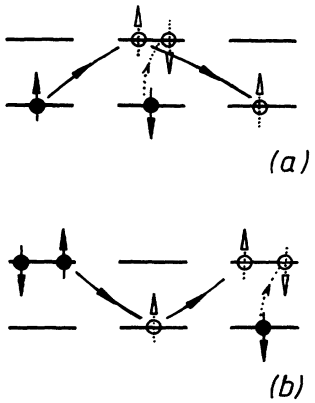


FIG. 2. Effective electron hopping in the (a) lower and (b) upper quasiparticle subband.

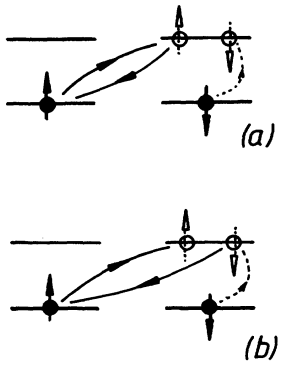


FIG. 3. Elementary processes for the kinetic exchange (a) without and (b) with spin flip.

quasiparticle subband. This includes, e.g., even processes like those in Figs. 2(a) and 2(b). Figure 2(a) can be ascribed to an "effective" hopping in the lower, Fig. 2(b) to an "effective" hopping in the upper quasiparticle subband. The transient virtual intersubband transitions lead to a certain renormalization of quasiparticle energies and lifetimes. There are, however, special intersubband transitions, which are by no means ascribable to an effective *intraband* hopping. Such processes are sketched in Fig. 3. A $\sigma$ electron jumps first from the otherwise unoccupied site $\mathbf{R}_{i\alpha}$ to site $\mathbf{R}_{j\beta}$, which is already singly occupied by an electron with opposite spin $-\sigma$. In the next step one of the two electrons, which are now at $\mathbf{R}_{j\beta}$, hops back to $\mathbf{R}_{i\alpha}$. In Fig. 3(a), the $\sigma$ electron comes back, so that the initial situation is restored. In Fig. 3(b), a spin exchange between $\mathbf{R}_{i\alpha}$ and $\mathbf{R}_{j\beta}$ occurs.

We decide to restrict $H_U^{(1)}(m)$ to processes such as those in Fig. 3, which finally will provide an effective spin coupling between particles at $\mathbf{R}_{i\alpha}$ and $\mathbf{R}_{j\beta}$. We extract such terms by a canonical transformation,[28] details of which are elaborated on in Appendix A. We restrict ourselves here to a listing of the final equations:

$$H_{3d}+H_{3d}^{(U)}=\sum_m H_U(m)$$
$$=H_{3d}^{(0)}+H_{3d}^{(1)}+H_{3d}^{(2)}+H_{3d}^{(\mathrm{ex})} . \tag{2.23}$$

As required, the operator $H_{3d}^{(0)}$ describes the quasiparticle propagation within the two Hubbard-split bands:

$$H_{3d}^{(0)}=\sum_{i,j,\sigma,\alpha,\beta,m}[T_{ij}^{\alpha\beta}(m)(1-n_{i\alpha m-\sigma})c_{i\alpha m\sigma}^{\dagger}c_{j\beta m\sigma}(1-n_{j\beta m-\sigma})+(T_{ij}^{\alpha\beta}(m)+\tfrac{1}{2}U\delta_{ij}\delta_{\alpha\beta})n_{i\alpha m-\sigma}c_{i\alpha m\sigma}^{\dagger}c_{j\beta m\sigma}n_{j\beta m-\sigma}] . \tag{2.24}$$

The other terms in (2.23) result from virtual intersubband transitions leading to effective exchange integrals of the form

$$J_{ij}^{\alpha\beta}(m)=-\frac{1}{U}(T_{ij}^{\alpha\beta}(m))^2(1-\delta_{ij}\delta_{\alpha\beta}) . \tag{2.25}$$

The partial operator $H_{3d}^{(1)}$ provides a spin-independent interaction between singly occupied lattice sites. However, because of its spin independence, this term will be rather unimportant where magnetic phenomena is concerned:

$$H_{3d}^{(1)}=\tfrac{1}{4}\sum_{i,j,\alpha,\beta,m}J_{ij}^{\alpha\beta}(m)\nu_{i\alpha m}\nu_{j\beta m} . \tag{2.26}$$

The operator $\nu_{i\alpha m}$ may be considered, correspondingly, as a spin-independent number operator for singly occupied sites:

$$\nu_{i\alpha m}=\sum_{\sigma}(1-n_{i\alpha m-\sigma})n_{i\alpha m\sigma} . \tag{2.27}$$

The third partial operator $H_{3d}^{(2)}$ in (2.23) contributes only if the system contains simultaneously doubly occupied and completely empty sites, a situation which is highly unlikely in strongly correlated systems, and that independently of the actual degree of band filling:

$$H_{3d}^{(2)}=-\tfrac{1}{2}\sum_{\substack{i,j,\sigma,m,\\ \alpha,\beta}}J_{ij}^{\alpha\beta}(m)[\,n_{i\alpha m\sigma}n_{i\alpha m-\sigma}\times(1-n_{j\beta m\sigma})(1-n_{j\beta m-\sigma})+c_{i\alpha m\sigma}^{\dagger}c_{i\alpha m-\sigma}^{\dagger}\times c_{j\beta m-\sigma}c_{j\beta m\sigma}] . \tag{2.28}$$

Besides $H_{3d}^{(0)}$, which is defined in (2.24), the most decisive part of (2.23) is $H_{3d}^{(\mathrm{ex})}$:

$$H_{3d}^{(\mathrm{ex})}=-\sum_{i,j,\alpha,\beta,m}J_{ij}^{\alpha\beta}(m)\boldsymbol{\sigma}_{i\alpha m}\cdot\boldsymbol{\sigma}_{j\beta m} . \tag{2.29}$$

It represents an effective exchange coupling between localized spins, which may give rise to the above-mentioned collective spin excitations. The spin operators $\boldsymbol{\sigma}$ are introduced in Eq. (2.16).

Since we are excludingly interested in the strong-coupling limit $U\gg W_m$, not all parts of the Hamiltonian

(2.23) are of the same importance. All terms in $H_{3d}^{(1,2)}$ are of order $W_m^2/U$ and thereby small compared to those in $H_{3d}^{(0)}$. Furthermore, we already recognized that they are of only minor relevance to the interesting magnetic and electronic properties of the Mott insulators. We therefore simplify them from the very beginning in a Hartree-Fock manner. If we define

$$J_{\mathbf{q}}^{\alpha\beta}(m)=\frac{1}{N}\sum_{i,j}J_{ij}^{\alpha\beta}(m)\exp[-i\mathbf{q}\cdot(\mathbf{R}_i-\mathbf{R}_j)]\ , \tag{2.30}$$

$$J_{\mathbf{q}}(m)=J_{\mathbf{q}}^{\alpha\alpha}(m),\quad K_{\mathbf{q}}(m)=J_{\mathbf{q}}^{\alpha\bar{\alpha}}(m)$$
$$(\alpha=A,B\Longleftrightarrow\bar{\alpha}=B,A)\ , \tag{2.31}$$

and renormalize the hopping integrals in (2.24),

$$\tilde{T}_{ij}^{\alpha\beta}(m)=T_{ij}^{\alpha\beta}(m)(1-\delta_{ij}\delta_{\alpha\beta})+\tilde{T}_0(m)\delta_{ij}\delta_{\alpha\beta}\ , \tag{2.32}$$

by replacing the old center of gravity $T_0(m)$ by

$$\tilde{T}_0(m)=T_0(m)+\tfrac{1}{2}\langle\hat{n}_m\rangle[J_0(m)+K_0(m)]\ , \tag{2.33}$$

and change the Coulomb matrix element $U$ into

$$\tilde{U}_m=U-[J_0(m)+K_0(m)]\cong U\ , \tag{2.34}$$

then $H_{3d}^{(1)}$ and $H_{3d}^{(2)}$ are completely absorbed by $H_{3d}^{(0)}$ in (2.24).

Eventually we get the following final version of the $3d$ partial system in our model Hamiltonian (2.5):

$$H_{3d}+H_{3d\text{-}3d}=H_{3d}^{(0)}+H_{3d}^{(\mathrm{ex})}+H_{3d}^{(J)}+H_{3d}^{(\bar{U})}\ . \tag{2.35}$$

The interband interactions $H_{3d}^{(J)}$ and $H_{3d}^{(\bar{U})}$ are given by (2.17) and (2.18), respectively. $H_{3d}^{(0)}$ expresses the quasiparticle propagation within the Hubbard-split bands (2.24), while $H_{3d}^{(\mathrm{ex})}$ brings into play collective spin excitations via kinetic exchange (2.29).

## III. EFFECTIVE-MEDIUM APPROACH

### A. Formal solution

Our theoretical model for transition-metal monoxides such as NiO, CoO, FeO, and MnO is established by the operators (2.5) and (2.35). It goes without saying that the corresponding many-body problem cannot be treated rigorously. Approximations must be tolerated. Special complications are due to the physically decisive $3d$-electron interactions in (2.35). Their influence results in a rather involved self-energy contribution $M_{ij\sigma}^{\alpha\beta}(E;m)$ for the band electrons. The operator (2.35) is composed of four partial operators. All, except for $H_{3d}^{(\bar{U})}$, are well known from simpler models of magnetism ($H_{3d}^{(0)}$, split-band Hubbard model; $H_{3d}^{(\mathrm{ex})}$, Heisenberg model; $H_{3d}^{(J)}$, $s$-$f$ model). Each of the four partial operators contributes in a special manner to the self-energy $M_{ij\sigma}^{\alpha\beta}(E;m)$, which thus can be decomposed accordingly:

$$M_{ij\sigma}^{\alpha\beta}(E;m)=\sum_{y}[M_{ij\sigma}^{\alpha\beta}(E;m)]^{(y)}\ ,$$
$$\text{with } y=0,\ \text{ex},\ J,\ \text{or}\ \bar{U}\ . \tag{3.1}$$

The superscript $y$ numbers in an obvious way the contributions of the four partial operators. Let us assume for the moment that all self-energy parts except for $[M_{ij\sigma}^{\alpha\beta}(E;m)]^{(x)}$ are already known, so that we can define the following effective one-particle energies,

$$[T_{ij\sigma}^{\alpha\beta}(E;m)]^{(x)}=T_{ij}^{\alpha\beta}(m)+\sum_{y\ (\neq x)}[M_{ij\sigma}^{\alpha\beta}(E;m)]^{(y)}\ , \tag{3.2}$$

by which an effective-medium Hamiltonian is introduced:

$$\hat{H}_{3d}^{(x)}=\sum_{\substack{i,j,\sigma,\\ \alpha,\beta,m}}[T_{ij\sigma}^{\alpha\beta}(E;m)]^{(x)}c_{i\alpha m\sigma}^{\dagger}c_{j\beta m\sigma}+H_{3d}^{(x)}\ . \tag{3.3}$$

This Hamiltonian is energy dependent and possibly non-Hermitian, since the self-energy parts $[M_{ij\sigma}^{\alpha\beta}(E;m)]^{(y)}$ in (3.2) may be complex functions. However, the decisive one-electron Green function (3.7), from which we shall get all needed information about the underlying physical system, does not change at all when (2.35) is replaced by $\hat{H}_{3d}^{(x)}(E)$. On the other hand, the remaining many-body problem posed by (3.3) is formally simpler than the original one because only one of the four interaction terms appears explicitly. For $x=U$ we have to solve an "effective" Hubbard problem, for $x=J$ an "effective" $s$-$f$ problem and so on. The corresponding models of magnetism have been studied intensively in the past, so that reliable approaches are available. Applying such an approach to the "effective $x$ problem" given by $\hat{H}_{3d}^{(x)}(E)$ provides us with the general structure of the corresponding self-energy part $[M_{ij\sigma}^{\alpha\beta}(E;m)]^{(x)}$, and that in terms of the other self-energies $[M_{ij\sigma}^{\alpha\beta}(E;m)]^{(y\neq x)}$. Furthermore, the result will contain various expectation values, among them, e.g., the important spin-dependent average occupation numbers $\langle n_{\alpha m\sigma}\rangle$:

$$[M_{ij\sigma}^{\alpha\beta}(E;m)]^{(x)}$$
$$=\mathcal{F}_x(E;m|[M_{ij\sigma}^{\alpha\beta}(E;m)]^{(y\neq x)},\langle\cdots\rangle)\ . \tag{3.4}$$

It is a key point of our theory that all these expectation values must be exactly expressable by the one-electron Green function (or by the respective spectral density) of the *full* system. This procedure is repeated for all four self-energies $[M_{ij\sigma}^{\alpha\beta}(E;m)]^{(x)}$ leading finally to a closed system of equations which can be solved self-consistently. The actual approaches we used for the various self energy parts are discussed step by step in the subsequent sections.

As soon as we have approximately derived in the above-described manner the self-energy (3.1), we can express without further simplifications the basic one-electron Green function in terms of this quantity. For this purpose we first write, for abbreviation,

$$D_{m\sigma}^{\alpha\beta}(\mathbf{k},E)=E\delta_{\alpha\beta}-\varepsilon_m^{\alpha\beta}(\mathbf{k})-M_{\mathbf{k}\sigma}^{\alpha\beta}(E;m)\ , \tag{3.5}$$

$$F_{\mu}^{\alpha\beta}(\mathbf{k},E)=E\delta_{\alpha\beta}-\varepsilon_{\mu}^{\alpha\beta}(\mathbf{k})\ , \tag{3.6}$$

where $M_{\mathbf{k}\sigma}^{\alpha\beta}(E;m)$ is the Fourier transform of the self-energy (3.1). The total Green-function matrix for the altogether eight subbands in two sublattices may be represented in the following compact form:

$$\{[G_{\mathbf{k}\sigma}(E)]\}^{-1}=\begin{pmatrix} G^{AA}_{\mathbf{k}\sigma}(E) & G^{AB}_{\mathbf{k}\sigma}(E) \\ G^{BA}_{\mathbf{k}\sigma}(E) & G^{BB}_{\mathbf{k}\sigma}(E) \end{pmatrix}^{-1} = \begin{pmatrix} P^{AA}_{\mathbf{k}\sigma}(E) & P^{AB}_{\mathbf{k}\sigma}(E) \\ P^{BA}_{\mathbf{k}\sigma}(E) & P^{BB}_{\mathbf{k}\sigma}(E) \end{pmatrix} . \tag{3.7}$$

$P^{\alpha\beta}_{\mathbf{k}\sigma}(E)$ is an $8\times 8$ matrix which consists of four blocks

$$P^{\alpha\beta}_{\mathbf{k}\sigma}(E)=\begin{pmatrix} A^{\alpha\beta}_{\mathbf{k}\sigma}(E) & \hat{V}^{\alpha\beta}_{\mathbf{k}} \\ (\hat{V}^{\alpha\beta}_{\mathbf{k}})^T & B^{\alpha\beta}_{\mathbf{k}}(E) \end{pmatrix} . \tag{3.8}$$

$A^{\alpha\beta}_{\mathbf{k}\sigma}(E)$ and $B^{\alpha\beta}_{\mathbf{k}}(E)$ are diagonal matrices:

$$A^{\alpha\beta}_{\mathbf{k}\sigma}(E)=[D^{\alpha\beta}_{m\sigma}(\mathbf{k};E)\delta_{mn}]_{\substack{m=1,\ldots,5;\\ n=1,\ldots,5}} , \tag{3.9}$$

$$B^{\alpha\beta}_{\mathbf{k}}(E)=[F^{\alpha\beta}_{\mu}(\mathbf{k};E)\delta_{\mu\nu}]_{\substack{\mu=1,2,3;\\ \nu=1,2,3}} . \tag{3.10}$$

$\hat{V}^{\alpha\beta}_{\mathbf{k}}$ is a $5\times 3$ matrix which provides the influence of the $3d$-$2p$ hybridization:

$$\hat{V}^{\alpha\beta}_{\mathbf{k}}=-V^{\alpha\beta}_{\mathbf{k}}\begin{pmatrix} 1 & 1 & 1 \\ 1 & 1 & 1 \\ 1 & 1 & 1 \\ 1 & 1 & 1 \\ 1 & 1 & 1 \end{pmatrix} . \tag{3.11}$$

A matrix inversion in (3.7) finally yields the Green-function matrix, the diagonal elements of which determine the quasiparticle density of states (Q-DOS). For sublattice $\alpha$ and spin $\sigma$ holds

$$\rho_{\alpha\sigma}(E)=-\frac{1}{\pi}\mathrm{Im}\frac{1}{N}\sum_{\mathbf{k}}\left[\sum_{m=1}^{5}[G_{\mathbf{k}\sigma}(E+i0^+)]^{\alpha\alpha}_{mm}+\sum_{\mu=1}^{3}[G_{\mathbf{k}\sigma}(E+i0^+)]^{\alpha\alpha}_{\mu\mu}\right]$$
$$=\sum_{m=1}^{5}\rho_{\alpha m\sigma}(E)+\sum_{\mu=1}^{3}\rho_{\alpha\mu\sigma}(E) . \tag{3.12}$$

It is our main task to determine this important function for *all* temperatures and band occupations. We notice that the decomposition of the chemical lattice into sublattices still allows different magnetic configurations, namely, paramagnetism, ferromagnetism, and antiferromagnetism:

$$\rho_{A\sigma}(E)=\rho_{B\sigma}(E), \quad \text{paramagnetism, ferromagnetism} , \tag{3.13}$$

$$\rho_{A\sigma}(E)=\rho_{B-\sigma}(E), \quad \text{antiferromagnetism} . \tag{3.14}$$

All expectation values which enter the above-discussed self-energy parts $[M^{\alpha\beta}_{ij\sigma}(E;m)]^{(x)}$ are rigorously expressable by the Green function (3.7) or the Q-DOS leading thereby, together with Eqs. (3.1)–(3.12), to a closed system of equations, which we evaluate, e.g., for the spin-dependent average occupation numbers per site:

$$\langle n_{\alpha\sigma}\rangle=\int_{-\infty}^{+\infty}dE\,\rho_{\alpha\sigma}(E)\{\exp[\beta(E-\mu)]+1\}^{-1} . \tag{3.15}$$

They indicate the appearance of spontaneous magnetism by $\langle n_{\alpha\sigma}\rangle\neq\langle n_{\alpha-\sigma}\rangle$. For the self-consistent solution of our model, the stability of any magnetic configuration mainly depends on the relative strength of the Coulomb coupling constants $U$, $\bar{U}$, and $J$. Very important parameters are furthermore the $3d$-electron density, the temperature, and the lattice structure. In this paper we shall concentrate on parameter constellations which are relevant for the transition-metal monoxides. In the following subsections we explicitly derive the self-energy parts $[M^{\alpha\beta}_{ij\sigma}(E;m)]^{(x)}$.

### B. Interband self-energy contributions

In Ref. 25, a self-consistent Green-function decoupling is used for an approximate solution of the many-body problem posed by the Hamiltonian $H^{(J)}_{3d}$, which is identical to the interaction part of the $s$-$f$ model.[23] This method correctly reproduces all exactly solvable, nontrivial limiting cases of the $s$-$f$ model. Furthermore, it contributes to an astonishingly realistic description of the band ferromagnet Ni. The resulting self-energy consists of two parts:[25]

$$[M^{\alpha\beta}_{\mathbf{k}\sigma}(E;m)]^{(J)}=-\tfrac{1}{2}z_\sigma J\delta_{\alpha\beta}\sum_{m'\sigma'}^{m'\neq m}z_{\sigma'}\langle n_{i\alpha m'\sigma'}\rangle + \tfrac{1}{4}J^2F^{\alpha\beta}_{m\sigma}(E) . \tag{3.16}$$

$F^{\alpha\beta}_{m\sigma}(E)$ is a very complicated functional of energy, which stems from spin-exchange processes between the band electron and the effective localized spins, defined in (2.18). For details of the mathematical derivation, the reader is referred to Ref. 25. In that paper it is shown for the band ferromagnet Ni that this effective electron-magnon scattering gives rise to some kind of irregular temperature behavior of the quasiparticle band states with a non-neglible influence on important magnetic data as, e.g., the Curie temperature. In the case of Mott insulators, however, we have to assume that the interband exchange coupling is at least 1 order of magnitude smaller than the intraband matrix element $U$ and the direct interband Coulomb interaction $\bar{U}$, respectively.[29] We therefore believe that $H^{(J)}_{3d}$ is only of minor importance with respect to the striking phenomenon of Mott insulators. In a Hartree-Fock approximation, we therefore restrict the corresponding self-energy part to the first term in (3.16):

$$(M^{\alpha\beta}_{\mathbf{k}\sigma}(E;m)]^{(J)}\cong-\tfrac{1}{2}z_\sigma J\delta_{\alpha\beta}\sum_{m'\sigma'}^{m'\neq m}z_{\sigma'}\langle n_{i\alpha m'\sigma'}\rangle = M^{(J)}_{\alpha\sigma}(m)\delta_{\alpha\beta} . \tag{3.17}$$

We intend to investigate the detailed consequences of the electron-magnon scattering for the Mott insulators NiO, CoO, FeO, and MnO in a forthcoming paper. Additionally, it should be acceptable to simplify, in the same Hartree-Fock manner, the contribution of the direct interband interaction $H^{(\bar{U})}_{3d}$. That is, of course, not to be justified by a smallness of the coupling constant $\bar{U}$, but rather by its irrelevance with respect to magnetic phenomena:

$$[M^{\alpha\beta}_{\mathbf{k}\sigma}(E;m)]^{(\bar{U})} \cong \tfrac{1}{2}\bar{U}\delta_{\alpha\beta}\sum_{m'\sigma'}^{m'\neq m}\langle n_{i\alpha m'\sigma'}\rangle$$
$$= M^{(\bar{U})}_{\alpha}(m)\delta_{\alpha\beta} . \tag{3.18}$$

The expectation values in (3.17) and (3.18) are calculated self-consistently within the full model.

### C. Intraband quasiparticle propagation

The contribution of $H^{(0)}_{3d}$ to the electronic self-energy incorporates the "pure" intraband quasiparticle propagation. For its approximate determination we use a self-consistent spectral density approach (SDA), which we developed in previous papers[8,9,27] for the single-band Hubbard model. The general idea of this method is easily explained: The SDA starts from a two-pole ansatz for the one-electron spectral density, which is surely acceptable for pure intrasubband hopping in the strong-coupling regime $U \gg W_m$. The ansatz contains four at first unknown parameters, two quasiparticle energies with two related spectral weights. These four parameters are fitted to four exactly calculated spectral moments,[8] thereby guaranteeing that even processes such as those in Figs. 2(a) and 2(b) are properly taken into account. As already mentioned, both sketched situations may be interpreted as an "effective" electron propagation in the lower [Fig. 2(a)] and upper [Fig. 2(b)] quasiparticle subband, leading to a certain renormalization of quasiparticle energies and lifetimes.

The self-energy element $[M^{\alpha\alpha}_{\mathbf{k}\sigma}(E;m)]^{(0)}$ belongs to an electron hopping within the $\alpha$ sublattice. We determine the structure of this function by the just-mentioned self-consistent SDA, but refer the reader, for details of the actual evaluation, to our previous papers.[8,9,27] The nondiagonal elements of the self-energy matrix are obviously unimportant. They are exactly zero for paramagnetic and ferromagnetic systems, and thus unequal zero, if at all, for antiferromagnets *below* the Néel temperature $T_N$. According to Refs. 9 and 27 we therefore use

$$[M^{\alpha\beta}_{\mathbf{k}\sigma}(E;m)]^{(0)} = \delta_{\alpha\beta}\frac{\tilde{U}_m\langle n_{\alpha m-\sigma}\rangle(E-\langle B_{\alpha m-\sigma}\rangle)}{E-\langle B_{\alpha m-\sigma}\rangle-\tilde{U}_m(1-\langle n_{\alpha m-\sigma}\rangle)} . \tag{3.19}$$

With the aid of the one-electron spectral density

$$S^{\alpha\beta}_{\mathbf{k}\sigma}(E;m) = -\frac{1}{\pi}\mathrm{Im}[G^{\alpha\beta}_{\mathbf{k}\sigma}(E+i0^+)]^{\alpha\beta}_{mm} \tag{3.20}$$

and the general spectral theorem,[31] we get, for the average spin-dependent particle numbers, the well-known expression

$$\langle n_{\alpha m-\sigma}\rangle = \frac{1}{N}\sum_{\mathbf{k}}\frac{1}{\hbar}\int_{-\infty}^{+\infty}dE\, f_-(E)S^{\alpha\alpha}_{\mathbf{k}-\sigma}(E;m) . \tag{3.21}$$

$f_-(E)=\{\exp[\beta(E-\mu)]+1\}^{-1}$ is the Fermi function, and $\mu$ the chemical potential. Of decisive importance for the possibility of spontaneous ferromagnetism or antiferromagnetism is the second expectation value $\langle B_{\alpha m-\sigma}\rangle$ in the self-energy expression (3.19), which has the physical meaning of a spin-dependent band shift. It consists of higher correlation functions,[8,9]

$$\langle n_{\alpha m-\sigma}\rangle(1-\langle n_{\alpha m-\sigma}\rangle)[\langle B_{\alpha m-\sigma}\rangle - T_{0\alpha\sigma}(m)] = \frac{1}{N}\sum_{\substack{i,j,\beta\\[(i,\alpha)\neq(j,\beta)]}}[T^{\alpha\beta}_{ij-\sigma}(E;m)]^{(0)}\langle c^{\dagger}_{i\alpha m-\sigma}c_{j\beta m-\sigma}(2n_{i\alpha m\sigma}-1)\rangle , \tag{3.22}$$

which may lead, under certain conditions, to a relative shift of the spin subbands. Here we have written, for abbreviation,

$$T_{0\alpha\sigma}(m) = \tilde{T}_0(m) + M^{(\bar{U})}_{\alpha}(m) + M^{(J)}_{\alpha\sigma}(m) , \tag{3.23}$$

$\tilde{T}_0(m)$ is defined in (2.33). Fortunately, the higher correlation functions in (3.22) can rigorously be expressed by the one-electron spectral density (3.20), guaranteeing therewith a closed system of equations. The detailed recipe of how to do this has been presented in Refs. 9 and 27 so that we can restrict ourselves here to quote only the final result:

$$\langle n_{\alpha m-\sigma}\rangle(1-\langle n_{\alpha m-\sigma}\rangle)[\langle B_{\alpha m-\sigma}\rangle - T_{0\alpha\sigma}(m)] = \frac{1}{N}\sum_{\mathbf{k},\beta,\gamma}[\varepsilon^{\alpha\beta}_{m}(\mathbf{k})-\tilde{T}_0(m)\delta_{\alpha\beta}]\frac{1}{\hbar}\int_{-\infty}^{+\infty}dE\, f_-(E)$$
$$\times\left[\frac{2}{\tilde{U}_m}\{E\delta_{\gamma\alpha}-[\varepsilon^{\gamma\alpha}_{\mathbf{k}-\sigma}(E;m)]^{(0)}\}-\delta_{\gamma\alpha}\right]S^{\alpha\gamma}_{\mathbf{k}-\sigma}(E;m) . \tag{3.24}$$

$[\varepsilon^{\gamma\alpha}_{\mathbf{k}-\sigma}(E;m)]^{(0)}$ are the Fourier transforms ("effective Bloch energies") of the "effective" hopping integrals defined in (3.2). The same derivation, which led to (3.24), may also be used for the average number of singly occupied sites $\langle \nu_{\alpha m}\rangle$ (2.27), a quantity which is, of course, not really sublattice dependent:

$$\langle \nu_{\alpha m}\rangle = \langle \nu_m\rangle = \sum_{\sigma}\langle n_{i\alpha m\sigma}(1-n_{i\alpha m-\sigma})\rangle = \langle \hat{n}_{\alpha m}\rangle - 2\langle n_{\alpha m\sigma}n_{\alpha m-\sigma}\rangle . \tag{3.25}$$

We need this term at a later stage of our procedure. The higher expectation value on the right-hand side of (3.25) $\langle n_{am\sigma} n_{am-\sigma} \rangle$ can be recognized as a special case of the correlation functions in (3.22):

$$\langle \nu_m \rangle = \frac{1}{N} \sum_{k,\sigma,\gamma} \frac{1}{\hbar} \int_{-\infty}^{+\infty} dE\, f_-(E)(\delta_{\alpha\gamma} - (1/\tilde{U}_m)\{E\delta_{\gamma\alpha} - [\varepsilon_{m\sigma}^{\gamma\alpha}(\mathbf{k})]^{(0)}\}) S_{k\sigma}^{\alpha\gamma}(E;m) \ . \tag{3.26}$$

### D. Collective spin excitations

The final task is now to treat the kinetic exchange $H_{3d}^{(ex)}$ in (2.35). For this purpose we define the following retarded commutator Green function:[31]

$$L_{ij}^{\alpha\beta}(E;m) = \langle\langle \sigma_{iam}^{+}; \sigma_{j\beta m}^{-} \rangle\rangle_E \ . \tag{3.27}$$

This magnon part will be responsible for the appearance of collective spin excitations within our model. By use of the spectral theorem[31] we can derive with the magnon Green function the expectation value $\langle \sigma_{j\beta m}^{-} \sigma_{iam}^{+} \rangle$ and therewith the magnetization of the effective moment system:

$$\langle \sigma_{iam}^{z} \rangle = \tfrac{1}{2} \langle \nu_m \rangle - \langle \sigma_{iam}^{-} \sigma_{iam}^{+} \rangle \ . \tag{3.28}$$

Like the electronic self-energy parts, we determine the magnon Green function in its respective partial system, which is defined by the exchange term (2.29). A direct consequence of the fairly crude Hartree-Fock simplifications of $H_{3d}^{(J)}(m)$ and $H_{3d}^{(\tilde{U})}(m)$ in Sec. III B is the unrealistic neglect of any influence of the "other $d$ bands" on the "localized" spin in the $m$th subband $\sigma_{iam}$. We approximately reintroduce this influence by the staggered molecular field produced by the "other subbands,"

$$B_{i\alpha}(m) = B_\alpha(m) = 2 \sum_{m' (\neq m)} [J_0(m') - K_0(m')] \langle \sigma_{am'}^{z} \rangle \ , \tag{3.29}$$

by which we extend the exchange Hamiltonian (2.29):

$$H_{3d}^{(ex)}(m) = -\sum_{i,j,\alpha,\beta} J_{ij}^{\alpha\beta}(m)(\sigma_{iam}^{+}\sigma_{j\beta m}^{-} + \sigma_{iam}^{z}\sigma_{j\beta m}^{z}) + \sum_{i,\alpha} B_\alpha(m)\sigma_{iam}^{z} \ . \tag{3.30}$$

The equation of motion of $L_{ij}^{\alpha\beta}$ is straightforwardly derived:

$$[E - B_\alpha(m)] L_{ij}^{\alpha\beta}(E;m) = 2\delta_{ij}\delta_{\alpha\beta}\langle \sigma_{am}^{z} \rangle - 2 \sum_{l,\gamma} J_{il}^{\alpha\gamma}(m)(\langle\langle \sigma_{iam}^{z}\sigma_{l\gamma m}^{+}; \sigma_{j\beta m}^{-} \rangle\rangle_E - \langle\langle \sigma_{l\gamma m}^{z}\sigma_{iam}^{+}; \sigma_{j\beta m}^{-} \rangle\rangle_E) \ . \tag{3.31}$$

We simplify this equation by a random-phase approximation (RPA) decoupling similar to the so-called Tyablikov approximation[32] for the ferromagnetic counterpart, which is known to lead in that case to rather convincing results for low as well as high temperatures:[32]

$$\{E - B_\alpha(m) - 2\langle \sigma_{am}^{z} \rangle [J_0(m) - K_0(m)]\} L_{ij}^{\alpha\beta}(E;m) = 2\langle \sigma_{am}^{z} \rangle \left[\delta_{ij}\delta_{\alpha\beta} - \sum_{l,\gamma} J_{il}^{\alpha\gamma}(m) L_{lj}^{\gamma\beta}(E;m)\right] \ . \tag{3.32}$$

This equation is easily solved by Fourier transformation. With the abbreviations

$$E_{q\alpha}(m) = 2\langle \sigma_{am}^{z} \rangle Y_q(m) \ , \tag{3.33}$$

$$Y_q(m) = \{[X_q(m)]^2 - |K_q(m)|^2\}^{1/2} \ , \tag{3.34}$$

$$X_q(m) = J_q(m) - J_0(m) + K_0(m) + B_\alpha(m)/2\langle \sigma_{am}^{z} \rangle \ , \tag{3.35}$$

we get, for the diagonal elements of the Green-function matrix,

$$L_q^{\alpha\alpha}(E;m) = \frac{2\langle \sigma_{am}^{z} \rangle [E - 2\langle \sigma_{am}^{z} \rangle X_q(m)]}{[E - E_{q\alpha}(m)][E + E_{q\alpha}(m)]} \ . \tag{3.36}$$

The related magnon spectral density is obviously a two-pole function:

$$\hat{S}_q^{\alpha\alpha}(E;m) = \langle \sigma_{am}^{z} \rangle \{ [1 - X_q(m)/Y_q(m)]\delta(E - E_{q\alpha}(m)) + [1 + X_q(m)/Y_q(m)] \times \delta(E + E_{q\alpha}(m))\} \ . \tag{3.37}$$

The spectral theorem yields, in this case,

$$\langle \sigma_{iam}^{-}\sigma_{iam}^{+} \rangle = \frac{1}{N} \sum_q \int_{-\infty}^{+\infty} dE\, \hat{S}_q^{\alpha\alpha}(E;m)[\exp(\beta E) - 1]^{-1} = \langle \sigma_{am}^{z} \rangle \frac{1}{N} \sum_q [\phi_{q\alpha}^{(+)}(m) + \phi_{q\alpha}^{(-)}(m)] \ , \tag{3.38}$$

$$\phi_{q\alpha}^{(\pm)}(m) = [1 \mp X_q(m)/Y_q(m)]\{\exp[\pm\beta E_{q\alpha}(m)] - 1\}^{-1} \ . \tag{3.39}$$

Inserting (3.38) into (3.28) finally leads to the magnetization of the effective spin system:

$$\langle \sigma_{am}^{z} \rangle = \tfrac{1}{2}\langle \nu_m \rangle \left[1 + \frac{1}{N} \sum_q [\phi_{q\alpha}^{(+)}(m) + \phi_{q\alpha}^{(-)}(m)]\right]^{-1} \ . \tag{3.40}$$

The expectation value $\langle \nu_m \rangle$ is determined via (3.26) by the one-electron spectral density. Self-consistency is finally established via (2.16) which connects $\langle \sigma_{am}^{z} \rangle$ to the average particle numbers per site, $\langle n_{iam\sigma} \rangle$.

## IV. DISCUSSION OF THE RESULTS

Our present study aims specifically at the $3d$ transition-metal monoxides NiO, CoO, FeO, and MnO, which are known as prototypical Mott insulators. The other first-row transition-metal monoxides are not so interesting or not as appropriate for our model calculation. CaO ($n_{3d}=0$) and ZnO ($n_{3d}=10$) are ordinary nonmagnetic insulators, VO ($n_{3d}=3$) is a nonmagnetic metal, while CuO is an antiferromagnetic Mott insulator, which, however, does not possess the rocksalt structure. Therefore, we shall restrict ourselves to some brief comments on VO, CuO, and ZnO at the end of this section. From the experimental point of view, MnO,[33] NiO,[4,12,34] as well as CoO (Refs. 35–37) have been studied rather intensively, while the thermodynamically unstable FeO (Ref. 38) appears much less investigated.

The antiferromagnetic and insulating monoxides, except for CuO, all crystallize in the rocksalt structure, i.e., the $M^{2+}$ ions ($M$=Ni, Co, Fe, Mn) as well as the $O^{2-}$ ions occupy lattice sites of an fcc structure. As described in Sec. II A, as well as in Appendix A, we consider the fcc structure as built up by two chemically equivalent sublattices $A$ and $B$ in such a way that the (111) planes are ascribed in alternating sequence to $A$ and $B$, respectively. For paramagnetic, ferromagnetic, and nonmagnetic systems this decomposition is meaningless [$(A,\sigma)=(B,\sigma)$], while for antiferromagnets [$(A,\sigma)=(B,-\sigma)$] the so-called AF II type of transition-metal monoxides is realized. The Bloch density of states $\rho_{0m}(E)$, exhibited in Fig. 1, has been calculated in tight-binding approximation by an explicit $\mathbf{k}$-space summation over the first sublattice ("Bravais lattice") Brillouin zone, including nearest- and next-nearest-neighbor hopping. This holds for all $\mathbf{k}$ summations needed for the self-consistent solution of our model. Somewhat arbitrarily we have assumed that all $3d$ Bloch band have the same width ($W_m=W\ \forall m$), where the centers of gravity $T_{0m}$ are shifted against one another by 0.2 eV. The width $W$ is derived from the magnetic data of the $MO$ as described below. This arbitrariness will be removed in a forthcoming paper when we fix the Bloch energies by a full LSDA band-structure calculation. Here we are mainly interested in the general physical mechanism which causes the striking phenomena of the Mott insulators.

The Coulomb coupling constants have been estimated by Kanamori[30] for systems like NiO. In accordance with his findings,[2,3] we used, for all calculations,

$$U=13\ \text{eV},\quad \bar{U}=11\ \text{eV},\quad J=0.1\ \text{eV}\ . \tag{4.1}$$

$U$ is larger than that from the local-cluster calculation of Fujimori, Minami, and Sugano,[14] ($U=8-10$ eV), being, however, of the same order of magnitude. In any case, a direct comparison of the so-called "Hubbard $U$" must be problematic because of the use of different models. There does not appear in Ref. 14, e.g., a direct analogue to our $\bar{U}$. The comparatively small interband exchange $J$ may be a little bit surprising. However, it turns out that $J$ is rather unimportant for the striking phenomena of Mott insulators. A choice of $J=0.5$ eV, e.g., yields practically the same features. One has, additionally, to bear in mind that $J$ describes the exchange between two single $3d$ subbands. We shall see that the altogether effect of interband exchange in the degenerate $3d$ complex may amount to $\simeq 1$ eV.

A first general result of our self-consistent model evaluation is the fact that the characteristic properties of the Mott insulators are due to strong $M^{2+}$-$3d$-electron correlations. The oxygen $2p$ subbands partially overlap with some of the $3d$ quasiparticle subbands, therefore hybridizing with them. They are, however, in all cases completely filled and thus totally inactive with respect to the magnetism as well as to the conductivity properties of the monoxides.

As a further important general result, we find that, for the chosen set (4.1) of parameters and the assumed rocksalt structure, the ground state of the model systems is indeed antiferromagnetic for all $3d$-electron numbers per site $n_{3d}$ in between 5 (MnO) and 9 (CuO). As will be demonstrated below, this is due to the fact that, for such electron densities, at least one of the five $3d$ subbands is exactly half-filled. As is well known from previous model calculations,[8,9] such a situation strongly favors antiferromagnetism.

For fixed model parameters $U$, $\bar{U}$, $J$, and lattice struc-

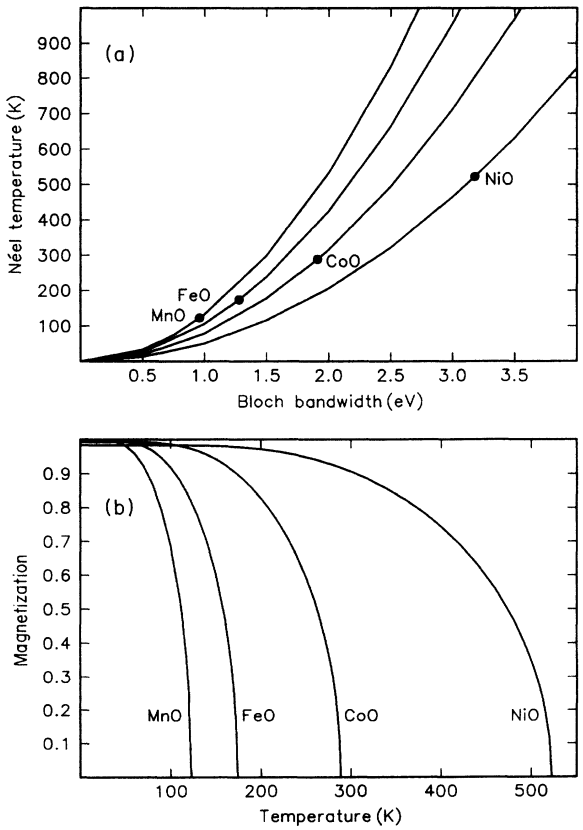


FIG. 4. (a) Néel temperature as function of Bloch bandwidth $W$ ($W_m=W\ \forall m$ in our model), for various integral values of band occupation $n_{3d}$ (8, NiO curve; 7, CoO curve; 6, FeO curve; 5, MnO curve). (b) Sublattice magnetization as function of temperature for the transition-metal monoxides.

ture, the magnetic and electric properties of the model system are decisively influenced by the band occupation $n_{3d}$ and the Bloch bandwidth $W$. Figure 4(a) shows the $W$ dependence of the Néel temperature $T_N$ for four different integral numbers:

$$n_{3d}=5\ (\Longleftrightarrow \mathrm{MnO}),\ 6\ (\Longleftrightarrow \mathrm{FeO}),\ 7\ (\Longleftrightarrow \mathrm{CoO}),\ 8\ (\Longleftrightarrow \mathrm{NiO})\ . \tag{4.2}$$

We have used the experimental values for the critical temperatures,[39]

$$T_N=122\ \mathrm{K}\ (\Longleftrightarrow \mathrm{MnO}),\ 175\ \mathrm{K}\ (\Longleftrightarrow \mathrm{FeO}),\ 289\ \mathrm{K}\ (\Longleftrightarrow \mathrm{CoO}),\ 523\ \mathrm{K}\ (\Longleftrightarrow \mathrm{NiO})\ , \tag{4.3}$$

to read off from the $T_N$-$W$ curves in Fig. 4(a) the following Bloch bandwidths:

$$W=0.96\ \mathrm{eV}\ (\Longleftrightarrow \mathrm{MnO}),\ 1.28\ \mathrm{eV}\ (\Longleftrightarrow \mathrm{FeO}),\ 1.91\ \mathrm{eV}\ (\Longleftrightarrow \mathrm{CoO}),\ 3.18\ \mathrm{eV}\ (\Longleftrightarrow \mathrm{NiO})\ . \tag{4.4}$$

Figure 4(b) shows our results for the temperature dependence of the sublattice magnetization of the four $3d$ transition-metal monoxides. They are normalized to the number of $3d$ holes, i.e., to get the total sublattice moment behavior we have to multiply the respective curve in Fig. 4(b) by $(10-n_{3d})\mu_B$. All curves look like Brillouin functions. The magnetizations for the sublattices $A$ and $B$ are, of course, different in sign but equal in magnitude, so that the total magnetization vanishes for all temperatures. As usual, for antiferromagnets the sublattices are not ferromagnetically saturated at $T=0$, i.e., the so-called "Néel state" with totally polarized sublattices is not the true ground state. The calculated $T=0$ moment of NiO, e.g., is, however, with $1.96\mu_B$ very close to that expected for a pure $3d^8(\mathrm{Ni}^{2+})$ configuration. The experimental value appears not very well established: $\mu(T=0)/\mu_B=1.64$,[40] 1.77,[41] 1.90.[42,43] In our self-consistent theory, the $T=0$ moment depends very sensitively on the molecular field $B_\alpha(m)$, defined in (3.29). Switching off tentatively, this field suppresses the NiO moment to some $1.65\mu_B$.

All these magnetic data are caused by a respective temperature behavior of the sublattice quasiparticle density of states (S-QDOS), which we are now going to discuss in detail. As already mentioned, the $3d$-$2p$ hybridization plays only a minor role as to the magnetic and insulating properties of the transition-metal monoxides. To illustrate as clearly as possible the decisive interrelations, we therefore discuss the S-QDOS first without hybridization. Figure 5 shows the S-QDOS $\rho_{\alpha m\sigma}(E)$ as function of energy for a parameter constellation valid for NiO, i.e., in particular $n_{3d}=8$, and that for various temperatures. The latter are chosen so that they belong to sublattice magnetizations which decrease step by step by about 20%. The solid lines are for the Ni $3d$ subbands, while dotted lines mark the O $2p$ subbands. There are three energy regions which are occupied by Ni $3d$ states, the lower two below, the uppermost above the chemical potential $\mu$. The gap between the uppermost and the intermediate Ni $3d$ part appears rather temperature independent, guaranteeing that NiO is insulating for all $T$. The three intermediate Ni $3d$ subbands are fully occupied, each with two electrons per site. Each of the two low-energy $3d$ quasiparticle subbands contains only one electron per site. The two unoccupied, high-energy $3d$ subbands are similarly built up by one quasiparticle state per site. This band structure, which simultaneously takes care for a permanent magnetic moment as well as for insulating behavior, can be understood as follows: The intraband Coulomb interaction $H_{3d}^{(U)}(m)$, which enters our model via (2.15), takes care for a splitting of each nondegenerate Bloch subband of the highly correlated electron system into two quasiparticle subbands. The energetic distance between the two subbands is roughly given by the intraband coupling constant $U$. This band separation turns out to be rather temperature independent. Each

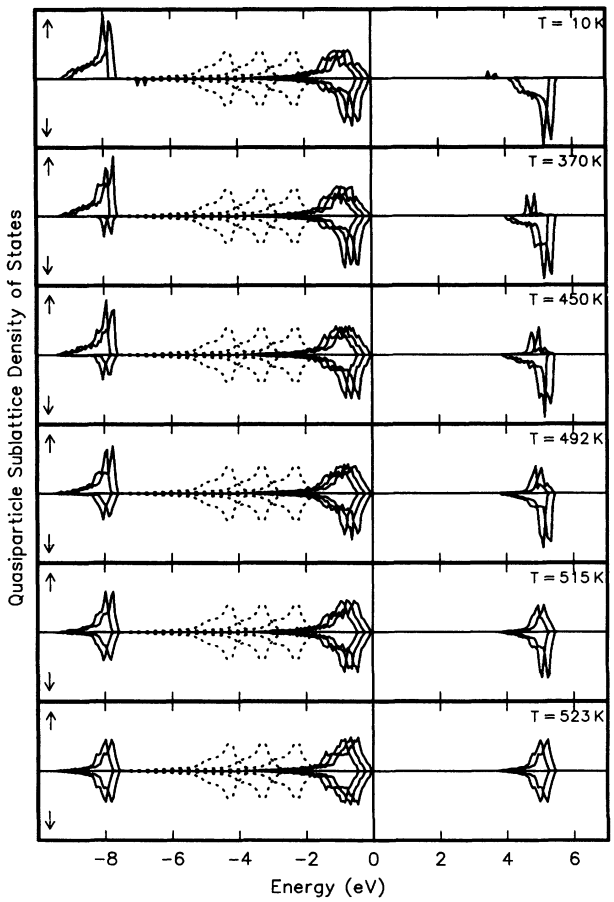


FIG. 5. Quasiparticle sublattice density of states $\rho_{Am\sigma}$ for NiO as function of energy for various temperatures. The latter are chosen so that, from top to bottom, the sublattice magnetization decreases step by step by about 20%. Note that $\rho_{Bm\sigma}(E)=\rho_{Am-\sigma}(E)$. The solid lines are for the Ni $3d$, the dotted lines are for the O $2p$ subbands. Hybridization $V=0$. Parameters as listed in (4.1).

quasiparticle subband has a spectral weight, which may simply be interpreted as the area under the respective Q-DOS curve. The total Q-DOS per spin and sublattice is normalized to one:

$$\int_{-\infty}^{+\infty} dE\, \rho_{\alpha m\sigma}(E)=1 \ . \tag{4.5}$$

The spectral weight of a quasiparticle subband depends on temperature $T$, band occupation $\langle n_{\alpha m}\rangle$, and electron spin $\sigma$. The $\sigma$ dependence is responsible for magnetic phenomena (see below), while the $\langle n_{\alpha m}\rangle$ dependence gives rise to two special cases. For empty Bloch bands ($\langle n_{\alpha m}\rangle=0$) the upper, and for completely filled Bloch bands ($\langle n_{\alpha m}\rangle=2$) the lower quasiparticle subband disappears. Transferred to the NiO case exhibited in Fig. 5, this means the following: three Ni $3d$ subbands are filled and thus do not have a lower quasiparticle subband. They are closely located to the also fully occupied oxygen $2p$ states. The other two Ni $3d$ subbands are exactly half-filled, and therefore splitted by an energy amount of order $U$. The two lower quasiparticle bands are below the chemical potential $\mu$, the two upper bands above. We conclude, that the unoccupied high-energy and the occupied low-energy part of the Ni $3d$ spectrum belong together, arisen out of an electron-correlation-caused quasiparticle splitting. They are often denoted in literature as "Hubbard subbands." In the language of photoemission spectroscopy,[5,43] the lower Hubbard band is built up by $3d^7$ states, observable by XPS, while the $3d^9$ states form the upper Hubbard subband [bremsstrahlung-isochromat spectroscopy (BIS)]. In addition, photoemission experiments reveal so-called $3d^8L^{-1}$ states[5,43] in the intermediate-energy range. The self-consistent solution of our multiband model ascribes these $3d^8L^{-1}$ states to the three intermediate, fully occupied, Ni subbands, which strongly hybridize with the oxygen subbands. The optical gap of NiO is therefore not identical to the so-called "Hubbard gap." It is the energetic distance between the three fully occupied Ni bands and the two unoccupied upper quasiparticle subbands of the half-filled Ni bands. The frequently discussed nature of the insulator gap ($d$-$d$ or $p$-$d$?) is of only minor importance with respect to antiferromagnetism and Mott insulation. The $2p$-$3d$ hybridization, of course, exists and may take care for a sizable amount of $p$ character in the highest occupied states (see Fig. 13), but, in any case, this hybridization is not a necessary ingredient for an explanation of the basic mechanism in the transition-metal monoxides.

There remain two essential questions. What is the reason for the extraordinary "orbital polarization," i.e., why are the eight $Ni^{2+}$ electrons per site not homogeneously distributed over the five Ni $3d$ subbands? Why are the three fully occupied bands not located in the same energy region as the two unoccupied upper quasiparticle subbands, but rather some 4 eV below them? Both answers are given by the interband Coulomb interaction $H_{3d}^{(\bar{U})}(m)$, which enters our model via (2.19). This term may be interpreted as a somewhat "classical" Coulomb interaction between an electron from the $m$th subband and the charge densities of all the other subbands $m'\neq m$. According to (2.19) the corresponding coupling strength is mainly given by $\bar{U}$. A $Ni^{2+}$ electron in one of the fully occupied, intermediate subbands (Fig. 5) interacts via $\bar{U}$ with *six* electrons per site in other subbands, but not with the other electron in its own band. On the other hand, an electron in one of the two half-filled subbands "sees" *seven* electrons per site in other bands. The difference results in different subband positions. For $U$ and $\bar{U}$ values, as those in (4.1), it is energetically more favorable for the system to distribute the Ni $3d$ electrons not uniformly over the available subbands. It is this "classical" interband Coulomb interaction $\bar{U}$ which is decisively responsible for the insulating behavior of the transition-metal monoxides. The positions of the three energy regions, where Ni $3d$ are observable, hardly shift with temperature, thus guaranteeing the Mott insulation for arbitrary temperatures.

We note in passing that rather slight changes in the relative magnitude of $U$ and $\bar{U}$ can remove the above-mentioned "orbital polarization" resulting in a transition from an insulating to a metallic state. We speculate that this is the mechanism that causes the strikingly different behavior of transition-metal-oxides and transition-metal sulfides. There is no need to assume that the so-called "Hubbard $U$" changes from more than 10 eV to less than 2 eV when going from NiO to NiS. A detailed inspection of this interesting problem is in preparation.

The magnetic properties of the Mott insulator NiO are caused by an explicit spin dependence of the spectral weights below a critical temperature $T_N$. The three fully occupied Ni bands are magnetically inactive; they are only slightly spin split below $T_N$ because of the weak interband exchange $J$ with the magnetically active Ni bands. For very low temperatures (Fig. 5) the spectral weights of the lower quasiparticle subbands of the two half-filled Ni subbands are strongly spin dependent, namely, very close to one for $\sigma=\uparrow$ and very close to zero for $\sigma=\downarrow$. Exactly the opposite is true for the unoccupied upper quasiparticle subbands. With increasing temperature the weights of the lower $\downarrow$ bands as well as the upper $\uparrow$ bands become greater, leading to an increasing sublattice demagnetization. So the magnetization curve in Fig. 4(b) is not due to a firstly partial and finally complete overlap of respective spin bands, which, by the way, would make the insulator metallic, but rather by a temperature-dependent shift of quasiparticle states from an occupied low-energy to an unoccupied high-energy region and vice versa. One important consequence of this mechanism is that the insulating gap remains rather unaffected by the antiferromagnetic-paramagnetic phase transition, resolving thereby one of the most controversially discussed problems of the Mott insulators. It is worthwhile to point out that, in principle, the same mechanism helped us in Ref. 24 to understand the so-called "localized Heisenberg ferromagnetism" of the prototype EuO. We therefore agree with Brandow's formulation[2] that, in principle, Mott insulators can be classified as normal "magnetic insulators," in spite of the fact that the moment-carrying low-lying energy bands have a dispersion of up to 2 eV.

While Fig. 5 shows the NiO-sublattice quasiparticle density of states $\rho_{\alpha m\sigma}(E)$ separately for each $m$, we have

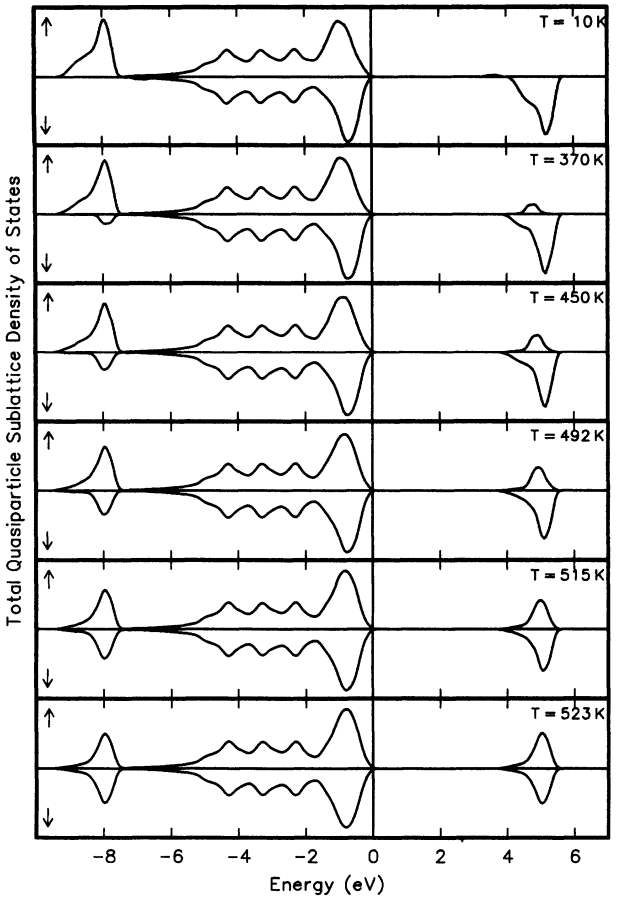


FIG. 6. The same as in Fig. 5 (NiO) but for the total sublattice QDOS $\rho_{A\sigma}(E)$, which has been folded with a Gaussian (FWHM=0.2 eV).

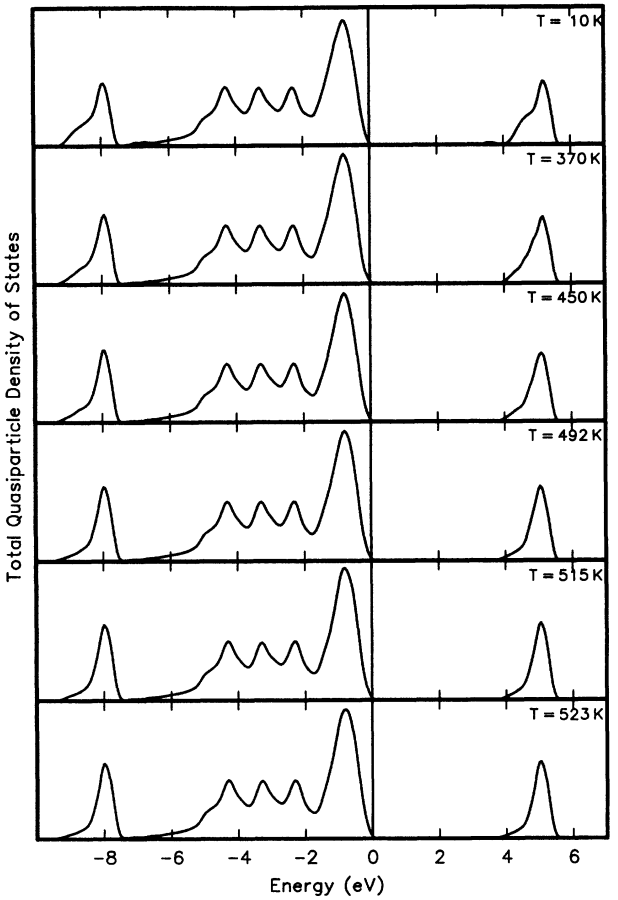


FIG. 7. The same as in Fig. 6 but now for the total quasiparticle density of states $\rho_\sigma(E)=\rho_{A\sigma}(E)+\rho_{B\sigma}(E)$.

summed up in Fig. 6 the partial S-QDOS to a total sublattice quasiparticle density of states as it should be observable in an appropriate neutron-scattering experiment. Unfortunately, a normal photoemission experiment is not capable to resolve the sublattice QDOS. Because of (3.14), however, the temperature effects in the sublattices $A$ and $B$ mutually compensate, so that the total Q-DOS of the antiferromagnets appears practically $T$ independent, as is exemplified in Fig. 7 for NiO. The relative order of the band states, however, agrees quantitatively with the available XPS and BIS data.[5]

Some LSDA band-structure calculations[6,7] are able to predict MnO and NiO as insulators at $T=0$ K by locating the Fermi edge within the Slater gap. Apart from the fact that this is a physically misleading interpretation of "Mott insulation," these calculations fail to reproduce the insulating behavior of CoO and FeO. Figure 8 shows that our model calculation yields, for all transition-metal monoxides, quite similar quasiparticle band structures. In the sequence NiO$\Longrightarrow$MnO, the number of fully occupied, intermediate $3d$ subbands decreases step by step by one, from three for NiO to zero for MnO, while the number of half-filled bands increases in the same direction from two to five. In any case, we find an insulator gap of some eV. Its origin is for all $MO$ exactly the same as explained above for the special case NiO. Since the magnetic moment, produced by the $(10-n_{3d})$ half-filled bands, increases from NiO to MnO, the exchange ($J$) caused spin splitting of the $(n_{3d}-5)$ fully occupied bands grows up in the same direction. We have used in Fig. 8 for all the transition-metal monoxides the same values for the Coulomb coupling constants as in (4.1) for NiO because here we are interested only in demonstrating the physical mechanism. In reality they may differ, being, however, for all monoxides surely of the same order of magnitude.

As already mentioned, CuO does not fit exactly our model assumptions because of a different crystal structure. However, when we disregard this fact, we find CuO, too, in agreement with the experiment to be an antiferromagnetic insulator ($n_{3d}=9$). Quite interesting is the case of VO with $n_{3d}=3$ electrons per site. All the five $3d$ subbands are less than half-filled. There do not appear completely filled quasiparticle subbands as for NiO, e.g., and therewith the intermediate $3d$ band region vanishes, so that the above-discussed orbital polarization, typical for the other $MO$, cannot occur. Furthermore, no magnetic ordering for less than half-filled energy bands is possible for a lattice with rocksalt structure (see the phase diagram in Ref. 9). The self-consistent solution of our model therefore predicts VO to be a nonmagnetic metal.

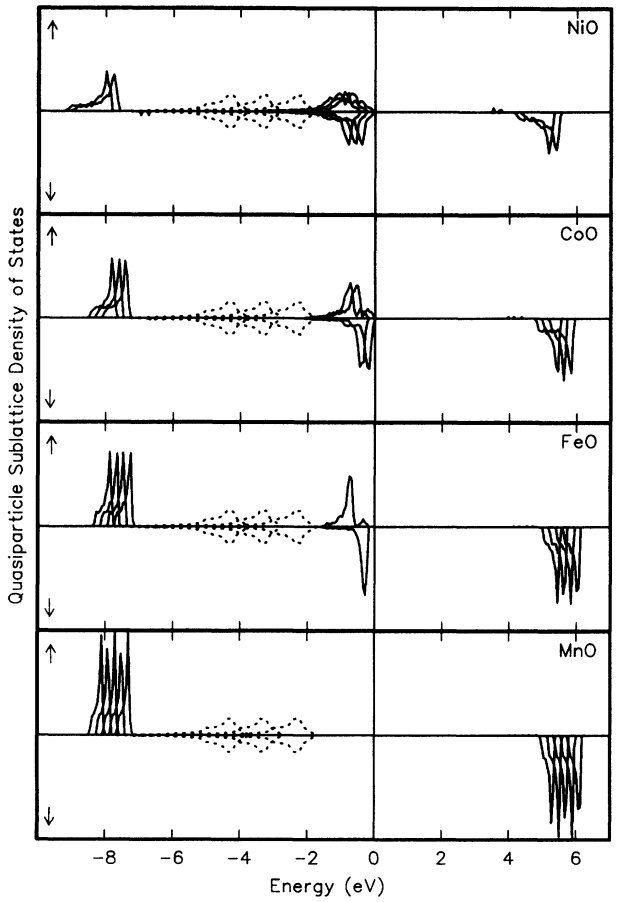


FIG. 8. Quasiparticle sublattice density of states at $T=10$ K for the various transition-metal monoxides as a function of energy. The solid lines are for the cation $3d$, the dotted lines are for the oxygen $2p$ subbands. Hybridization $V=0$, other parameters for all $MO$ as in (4.1).

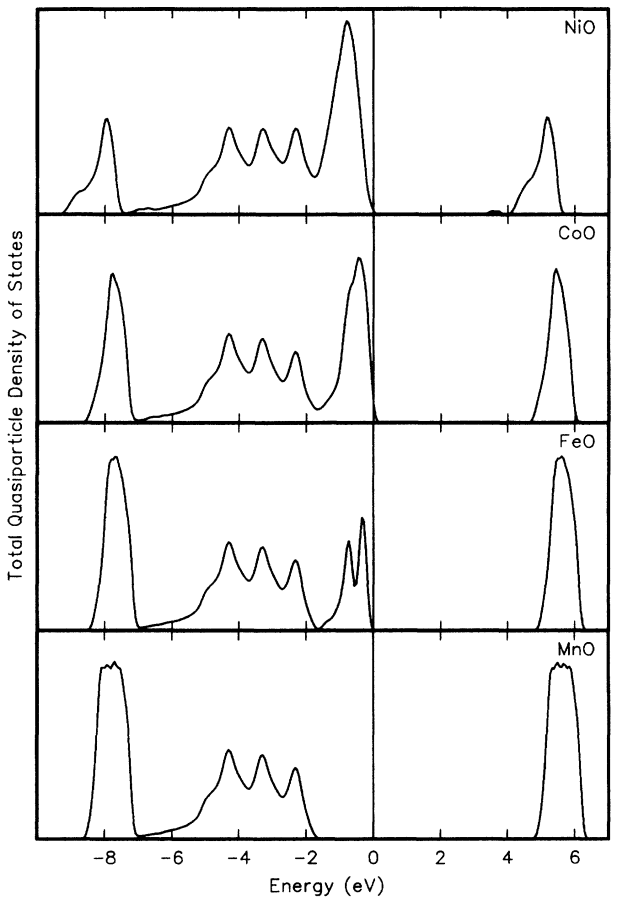


FIG. 9. The same as in Fig. 8 but now for the total quasiparticle density of states $\rho_\sigma(E)=\rho_{A\sigma}(E)+\rho_{B\sigma}(E)$, which has been folded with a Gaussian (FWHM=0.2 eV).

The total Q-DOS of the antiferromagnets (Fig. 9) turns out to be very similar for all the monoxides. From NiO to MnO, however, more and more of the intermediate $3d$ quasiparticle states ($\Longleftrightarrow 3d^8L^{-1}$) are removed, until this part vanishes for MnO. The states are shifted into the low-energy ($\Longleftrightarrow 3d^7$) and the unoccupied high-energy region ($\Longleftrightarrow 3d^9$).

Figure 10 shows the temperature behavior of the sublattice quasiparticle state density for CoO, which again exhibits a strong similarity to the NiO case in Fig. 5. The only difference lies in the above-discussed number of filled and half-filled subbands, respectively, and, of course, in the Néel temperature $T_N$. According to Fig. 4(a), the latter difference is caused by different Bloch bandwidths $W$ for NiO and CoO. We recognize, however, that the continuous decrease of the sublattice magnetization with increasing temperature happens exactly as analyzed above for NiO, namely, by a temperature-dependent shift of $\sigma$-quasiparticle states from an occupied low-energy to an unoccupied high-energy region, and vice versa for $(-\sigma)$ states. The insulator gap remains for CoO, too, practically unaffected by temperature variations.

It is a very important and illuminating experimental observation that the insulating behavior of transition-metal oxides is obviously bound to systems with an *integral* average number $n_{3d}$ of $3d$ electrons per site.[1,2] Slight deviations from stoichiometry are sufficient to make the $MO$ metallic. The valence mixing in $Fe_3O_4$ ($Fe^{2+}$,$Fe^{3+}$) causes metallic properties, although FeO and $Fe_2O_3$ are insulators. We have investigated this phenomenon within the framework of our theoretical model. An illustrative example of our self-consistent results is plotted in Fig. 11, where the energy dependence of the sublattice QDOS at $T=0$ K is plotted for various band occupations $7\leq n_{3d}\leq 8$. For clarity, only the active $3d$ subbands are represented. Furthermore, we have switched off, for computational simplicity, the kinetic exchange in (2.35), which is excludingly responsible for collective spin excitations, i.e., is very important for magnetic phenomena but plays a negligible role with regard to the conductivity problem. We note in passing that this "switching off" has an interesting side effect for the strongly correlated electron system under study. Our model solution yields, in such a case, an almost total spin polarization of the exactly half-filled $3d$ subbands, corresponding to a band version of the so-called Néel state. The kinetic exchange (2.29) and (3.30), respectively, which is "switched off" here, normally substantially

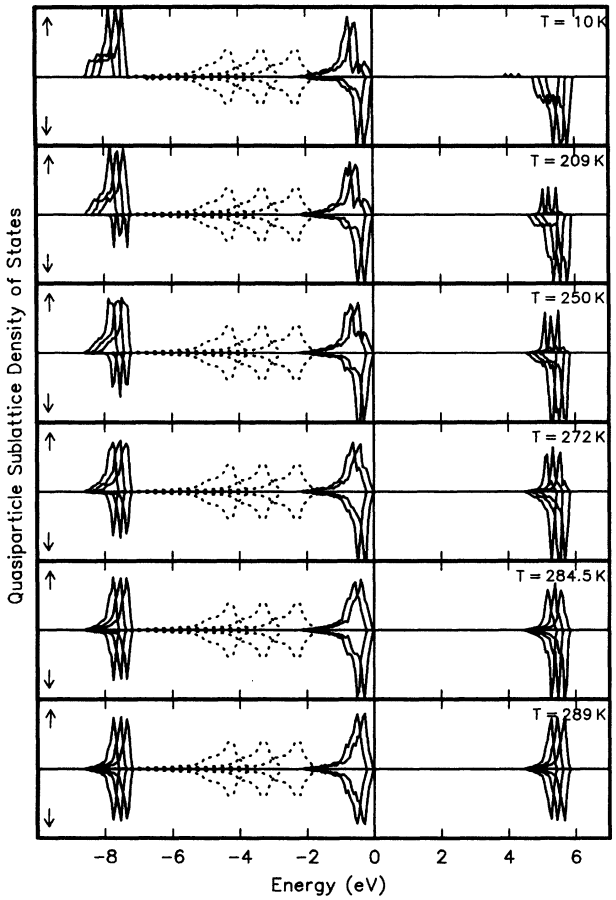


FIG. 10. Quasiparticle sublattice density of states $\rho_{Am\sigma}$ for CoO as function of energy for various temperatures. The latter are chosen so that, from top to bottom, the sublattice magnetization decreases step by step by about 20%. Note that $\rho_{Bm\sigma}(E)=\rho_{Am-\sigma}(E)$. The solid lines are for the Co $3d$, the dotted lines are for the O $2p$ subbands. Hybridization $V=0$. Parameters as listed in (4.1).

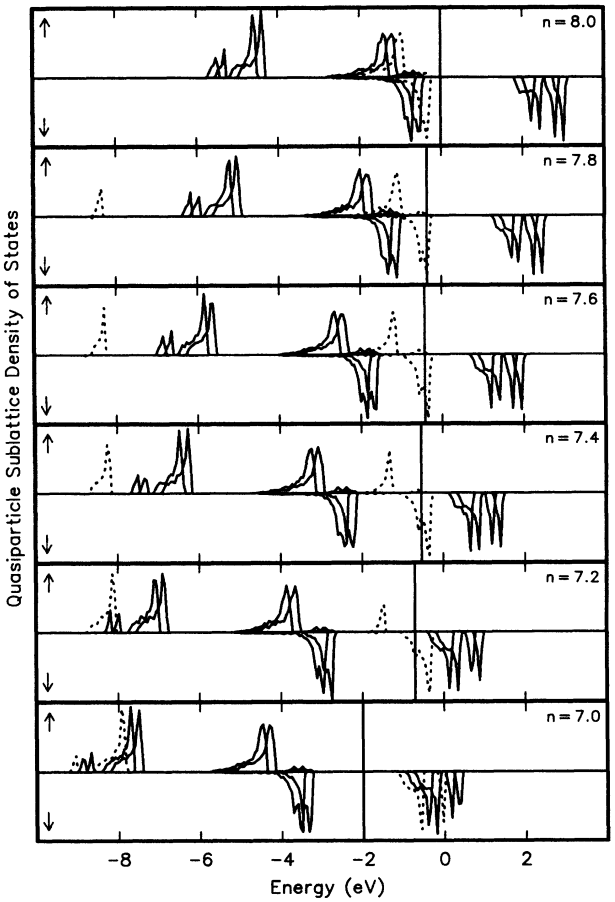


FIG. 11. Quasiparticle sublattice density of states as function of energy for various average numbers of $3d$ electrons per site between $n=8$ ($\Longleftrightarrow$NiO) and $n=7$ ($\Longleftrightarrow$CoO). The bars mark the position of the Fermi edge. Plotted are only the cation $3d$ subbands, and that for $T=0$ K. Parameters as in Fig. 5. The dotted lines are for the $3d$ subband, which decisively reacts on the change in band occupation. The system is an insulator for $n=7$ and 8 and becomes metallic for $n\neq 7,8$.

enhances the $T=0$ depolarization [see Fig. 4(b)]. As soon as total polarization happens ($\langle n_{\alpha m\sigma}\rangle_{T=0}=1$, $\langle n_{\alpha m-\sigma}\rangle_{T=0}=0$), the respective subband shows an additional "Slater splitting" (Fig. 11). We shall not comment on this splitting in more detail since it disappears immediately when the kinetic exchange is "switched on" again. We learn from Fig. 11 that, for the integer $n_{3d}=8$, the system consists of three fully occupied and two half-filled subbands consistent with the NiO case in Fig. 5. If we now slightly diminish the band occupation to $n_{3d}=7.8$, then the spin-$\downarrow$ part of one of the intermediate bands, marked in Fig. 11 as a dotted line, shifts partially above the Fermi edge. In the same moment a lower spin-$\uparrow$ quasiparticle band arises because the corresponding Bloch band is no longer completely filled. There is now a finite probability that a spin-$\uparrow$ electron of this band may jump onto a lattice site which is *not* preoccupied by a spin-$\downarrow$ electron of the same band. This fact manifests itself in the appearance of the lower "Hubbard band," the spectral weight of which is a direct measure of the just-mentioned probability. The latter increases with further decreasing band occupation. Analogously, the probability for a spin-$\uparrow$ electron to meet a spin-$\downarrow$ electron becomes smaller. As a consequence, the spectral weight of the lower spin-$\uparrow$ quasiparticle subband increases with decreasing $n_{3d}$ at cost of the weight of the upper spin-$\uparrow$ quasiparticle subband. The total area under the sublattice-QDOS is normalized to one (4.5). For $n_{3d}=7$, the spin-$\downarrow$ subband has moved completely above the Fermi edge, being, therefore, empty. This means that a spin-$\uparrow$ electron of the considered subband cannot meet a spin-$\downarrow$ electron to perform the intraband Coulomb interaction $U$. The upper spin-$\uparrow$ quasiparticle subband therefore disappears. For $n_{3d}=7$, the sublattice QDOS again exhibits a broad insulator gap of a few eV and becomes consistent with the CoO case represented in Fig. 10. For all noninteger values of $n_{3d}$, however, the Fermi edge falls into the band region provoking metallic behavior. Our model therefore confirms the experimental observation that "Mott insulation" is strictly bound to an integral number of $3d$ electrons with $5\leq n_{3d}\leq 9$. Figure

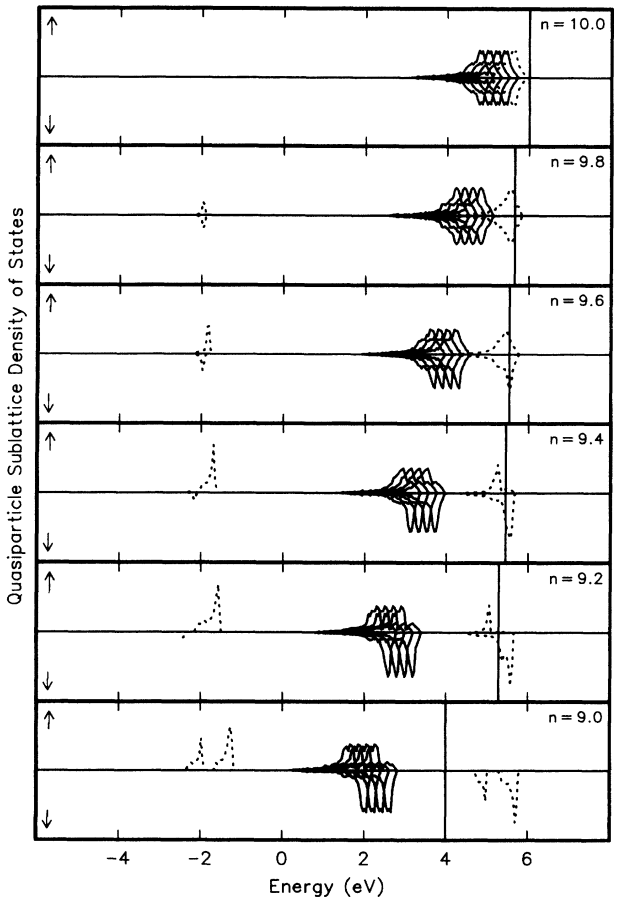


FIG. 12. The same as in Fig. 11 but now for $3d$-electron densities $9 \leq n_{3d} \leq 10$. $n_{3d}=9$ corresponds to CuO, $n_{3d}=10$ to ZnO.

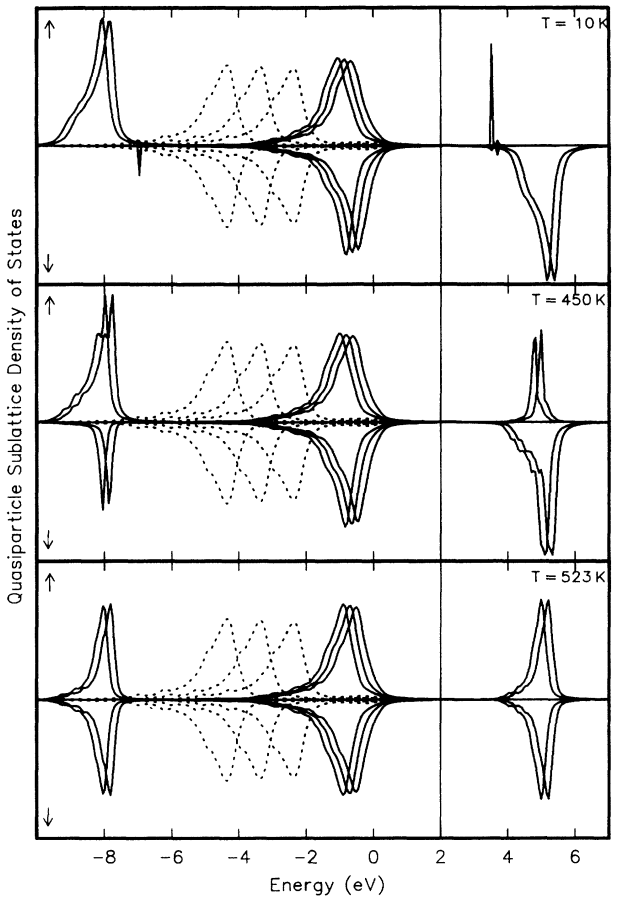


FIG. 13. Quasiparticle sublattice density of states $\rho_{Am\sigma}$ for NiO as a function of energy for three different temperatures. The solid lines are for the Ni $3d$, the dotted lines are for the O $2p$ subbands. This plot shall demonstrate the rather negligible influence of Ni $3d$–O $2p$ hybridization. ($V_{\mathbf{k}}^{\alpha\beta}=0.2$ eV.) Other parameters as listed in (4.1).

12 shows the insulator-metal transition for another example $9 \leq n_{3d} \leq 10$ (CuO $\Longrightarrow$ ZnO). Our model describes this transition as a typical many-body effect, being caused by a strong carrier-concentration dependence of the spectral weights of certain quasiparticle subbands.

So far the effects due to hybridization have been disregarded. We finally comment on the influence of this $3d$-$2p$ hybridization on the insulating and magnetic properties of Mott insulators, which turns out to be of only minor importance. Figure 13 shows, as an example, the quasiparticle sublattice density of states $\rho_{Am\sigma}(E)$ of NiO for three different temperatures, calculated with a hybridization $V_{\mathbf{k}}^{\alpha\beta}=0.2$ eV in (3.11). This is to compare with Fig. 5, where the same quantities are plotted without hybridization, while all the other parameters are identical. The special energetic positions of the $Ni^{2+}$ $3d$ quasiparticle bands compared to the $O^{2-}$ $2p$ subbands take care of the fact that hybridization effects are important only for the intermediate region, where the three fully occupied Ni $3d$ and the also fully occupied O $2p$ bands are located. One observes long, but fairly weak, subband tails. Although, strictly speaking, all subbands are occupying exactly the same energy regions because of finite hybridization, either the $d$ or the $p$ character strongly dominates everywhere. This, of course, depends on the actual mixing strength, which grows up with increasing overlap of the respective $3d$ quasiparticle subbands and the oxygen subbands. In any case, the top of the valence band ($\leftrightarrow 3d^8L^{-1}$) always has partial $p$ character. The main point is, however, that the characteristic phenomena, antiferromagnetism and Mott insulation, are completely unaffected by the hybridization. This remains true up to much higher $V_{\mathbf{k}}^{\alpha\beta}$ values than those we used for the results in Fig. 13. It is, however, to be expected that hybridization effects will be more evident via optical selection rules in angle-resolved photoemission. We are going to discuss such experiments in a forthcoming paper.

## ACKNOWLEDGMENT

Financial support of this work by the Deutsche Forschungsgemeinschaft (SFB 225) is gratefully acknowledged.

## APPENDIX A

The Bloch density of states $\rho_{0m}(E)$ for noninteracting electrons in the $m$th subband, represented in Fig. 1, is

calculated in the tight-binding approximation. The electron hopping $T_{ij}^{\alpha\beta}(m)$ is restricted to nearest ($\Delta_1^{\alpha\beta}$) and next-nearest neighbors ($\Delta_2^{\alpha\beta}$) in the chemical lattice

$$T_{ij}^{\alpha\beta}(m)=\begin{cases} T_0(m) & \text{if } \mathbf{R}_{i\alpha}=\mathbf{R}_{j\beta}\ , \\ T_1^{\alpha\beta}(m) & \text{if } \mathbf{R}_{i\alpha}=\mathbf{R}_{j\beta}+\Delta_1^{\alpha\beta}\ , \\ T_2^{\alpha\beta}(m) & \text{if } \mathbf{R}_{i\alpha}=\mathbf{R}_{j\beta}+\Delta_2^{\alpha\beta}\ , \\ 0 & \text{otherwise}\ . \end{cases} \tag{A1}$$

This means, for the Bloch energies $\varepsilon_m^{\alpha\beta}(\mathbf{k})$ defined in (2.7),

$$\varepsilon_m^{AA}(\mathbf{k})=\varepsilon_m^{BB}(\mathbf{k})=T_0(m)+T_1^{\alpha\alpha}(m)f_1(\mathbf{k}) +T_2^{\alpha\alpha}(m)f_2(\mathbf{k})=\varepsilon_m(\mathbf{k})\ , \tag{A2}$$

$$\varepsilon_m^{AB}(\mathbf{k})=[\varepsilon_m^{BA}(\mathbf{k})]^*=T_1^{AB}(m)g_1(\mathbf{k})+T_2^{AB}(m)g_2(\mathbf{k}) =t_m(\mathbf{k})\ . \tag{A3}$$

For the sublattice structure (AF II), explained in Sec. II A, the $\mathbf{k}$-dependent functions $f_{1,2}(\mathbf{k})$ and $g_{1,2}(\mathbf{k})$ are given by

$$f_1(\mathbf{k})=2\{\cos[(k_x-k_y)a/2]+\cos[(k_y-k_z)a/2] +\cos[(k_z-k_x)a/2]\}\ , \tag{A4}$$

$$f_2(\mathbf{k})=0\ , \tag{A5}$$

$$g_1(\mathbf{k})=2\{\cos[(k_x+k_y)a/2]+\cos[(k_y+k_z)a/2] +\cos[(k_z+k_x)a/2]\}\ , \tag{A6}$$

$$g_2(\mathbf{k})=2[\cos(k_xa)+\cos(k_ya)+\cos(k_za)]\ , \tag{A7}$$

$a$ is the Bravais lattice constant. The resulting Bloch density of states $\rho_{0m}(E)$ of the noninteracting electrons in the $m$th subband,

$$\rho_{0m}(E)=\frac{1}{2N}\sum_{\mathbf{k}}[\,\delta(E-\varepsilon_m(\mathbf{k})-|t_m(\mathbf{k})|) +\delta(E-\varepsilon_m(\mathbf{k})+|t_m(\mathbf{k})|)]\ , \tag{A8}$$

is plotted in Fig. 1 by use of $T_0(m)=0$, $T_2^{\alpha\alpha}(m)/T_1^{\alpha\alpha}(m)=1$, and a bandwidth of $W_m=1$ eV.

## APPENDIX B

For the explicit derivation of the partial Hamiltonian (2.23), we use a slight extension of the method proposed in Ref. 28. Since only two sites $\mathbf{R}_{i\alpha}$ and $\mathbf{R}_{j\beta}$ are involved, we can restrict our considerations first to a respective two-site model:

$$H_{ij}^{\alpha\beta}(m)=\sum_{\sigma}[\,T_{ij\sigma}^{\alpha\beta}(m)(c_{i\alpha m\sigma}^{\dagger}c_{j\beta m\sigma}+\text{H.c.}) +Un_{i\alpha m\sigma}n_{i\alpha m-\sigma}\delta_{ij}\delta_{\alpha\beta}]\ . \tag{B1}$$

At the end we simply have to sum over all indices $i,j,\alpha,\beta$:

$$H_U(m)=\tfrac{1}{2}\sum_{i,j,\alpha,\beta}H_{ij}^{\alpha\beta}(m)\ . \tag{B2}$$

We try to decompose the two-site Hamiltonian (B1) in complete analogy to (2.22). For this purpose we introduce projection operators $P_r(i\alpha,j\beta)$, $r=1,2$, which map the electron propagation onto the lower ($r=1$) and upper ($r=2$) quasiparticle sublevel. $P_1(i\alpha,j\beta)$, e.g., projects out situations, for which $\mathbf{R}_{i\alpha}$ and $\mathbf{R}_{j\beta}$ are, at most, singly occupied:

$$P_1(i\alpha,j\beta)=(1-n_{i\alpha m\sigma}n_{i\alpha m-\sigma})(1-n_{j\beta m\sigma}n_{j\beta m-\sigma})\ . \tag{B3}$$

$P_2(i\alpha,j\beta)$, on the other hand, picks out the cases for which at least one of the two sites is doubly occupied:

$$P_2(i\alpha,j\beta)=n_{i\alpha m\sigma}n_{i\alpha m-\sigma}(1-n_{j\beta m\sigma}n_{j\beta m-\sigma}) +n_{j\beta m\sigma}n_{j\beta m-\sigma}\ . \tag{B4}$$

It is easy to check that the so-defined projection operators fulfill the following conditions:

$$P_r^2(i\alpha,j\beta)=P_r(i\alpha,j\beta)\ , \tag{B5}$$

$$\sum_{r=1}^{2}P_r(i\alpha,j\beta)=1\ , \tag{B6}$$

$$P_1(i\alpha,j\beta)P_2(i\alpha,j\beta)=P_2(i\alpha,j\beta)P_1(i\alpha,j\beta)=0\ . \tag{B7}$$

These projection operators are now used for the formal decomposition of the two-site Hamiltonian:

$$H_{ij}^{\alpha\beta}(m)=(H_{ij}^{\alpha\beta})^{(0)}(m)+(H_{ij}^{\alpha\beta})^{(1)}(m)\ . \tag{B8}$$

The first term aims at quasiparticle hopping within the lower or within the upper levels,

$$(H_{ij}^{\alpha\beta})^{(0)}(m)=P_1(i\alpha,j\beta)H_{ij}^{\alpha\beta}(m)P_1(i\alpha,j\beta) +P_2(i\alpha,j\beta)H_{ij}^{\alpha\beta}(m)P_2(i\alpha,j\beta)\ , \tag{B9}$$

while the second term brings into play intersublevel transitions:

$$(H_{ij}^{\alpha\beta})^{(0)}(m)=P_1(i\alpha,j\beta)H_{ij}^{\alpha\beta}(m)P_2(i\alpha,j\beta) +P_2(i\alpha,j\beta)H_{ij}^{\alpha\beta}(m)P_1(i\alpha,j\beta)\ . \tag{B10}$$

In the next step we apply a canonical transformation to (B8):

$$\hat{H}_{ij}^{\alpha\beta}(m)=e^{-S}H_{ij}^{\alpha\beta}(m)e^{S} =(H_{ij}^{\alpha\beta})^{(0)}(m)+\{(H_{ij}^{\alpha\beta})^{(1)}+[(H_{ij}^{\alpha\beta})^{(0)}(m),S]_-\} +\tfrac{1}{2}(2[(H_{ij}^{\alpha\beta})^{(1)}(m),S]_-+[[(H_{ij}^{\alpha\beta})^{(0)}(m),S]_-,S]_-)+\text{higher-order terms}\ . \tag{B11}$$

The higher-order terms in the expansion may be neglected in the strong-coupling regime because $(H_{ij}^{\alpha\beta})^{(1)}$ as well as $S$ turn out to be of order $W_m^2/U$. $S$ is chosen in such a way that the first bracket in (B11) vanishes:

$$\{(H_{ij}^{\alpha\beta})^{(1)}+[(H_{ij}^{\alpha\beta})^{(0)}(m),S]_-\}=0\ . \tag{B12}$$

This means, for the transformed Hamiltonian,

$$\hat{H}_{ij}^{\alpha\beta}(m)=(H_{ij}^{\alpha\beta})^{(0)}+\tfrac{1}{2}[(H_{ij}^{\alpha\beta})^{(1)}(m),S]_- \ . \tag{B13}$$

Equation (B12) is used to fix the operator $S$. Multiplying from both sides with $P_r(i\alpha,j\beta)$, and exploiting Eqs. (B5)–(B7), (B9), and (B10), yields

$$P_r(i\alpha,j\beta)H_{ij}^{\alpha\beta}(m)\{P_r(i,\alpha;j,\beta)SP_r(i\alpha,j\beta)\}=\{P_r(i\alpha,j\beta)SP_r(i\alpha,j\beta)\}H_{ij}^{\alpha\beta}(m)P_r(i\alpha,j\beta) \quad (r=1,2) \ . \tag{B14}$$

This equation is solved by

$$P_r(i\alpha,j\beta)SP_r(i\alpha,j\beta)=\gamma P_r(i\alpha,j\beta) \quad (r=1,2) \tag{B15}$$

with an arbitrary constant $\gamma$. Multiplying (B12) from the left with $P_r$ and from the right with $P_{r'}$ with $r\neq r'$ leads to

$$\begin{aligned}P_r(i\alpha,j\beta)H_{ij}^{\alpha\beta}(m)P_{r'}(i\alpha,j\beta)=[\,&P_r(i\alpha,j\beta)S\{P_{r'}(i\alpha,j\beta)H_{ij}^{\alpha\beta}(m)P_{r'}(i\alpha,j\beta)\}\\&-\{P_r(i\alpha,j\beta)H_{ij}^{\alpha\beta}(m)P_r(i\alpha,j\beta)\}SP_{r'}(i\alpha,j\beta)] \ .\end{aligned} \tag{B16}$$

The expressions in the curly brackets correspond to an effective quasiparticle propagation in the lower ($r=1$) and upper ($r=2$) subband, suggesting, therefore, the following ansatz:

$$P_r(i\alpha,j\beta)H_{ij}^{\alpha\beta}(m)P_r(i\alpha,j\beta)=E_{ij}^{\alpha\beta}(r)P_r(i\alpha,j\beta) \ , \tag{B17}$$

where $E_{ij}^{\alpha\beta}(r)$ is a characteristic energy from the $r$th subband. From (B16) then follows

$$P_r(i\alpha,j\beta)SP_{r'}(i\alpha,j\beta)=\Delta_{ij}^{\alpha\beta}(r,r')P_r(i\alpha,j\beta)H_{ij}^{\alpha\beta}(m)P_{r'}(i\alpha,j\beta) \ , \tag{B18}$$

$$\Delta_{ij}^{\alpha\beta}(r,r')=[E_{ij}^{\alpha\beta}(r)-E_{ij}^{\alpha\beta}(r')]^{-1}\cong U^{-1} \ . \tag{B19}$$

With (B15) and (B18), inserted into (B13), the transformed operator now reads

$$\begin{aligned}\hat{H}_{ij}^{\alpha\beta}(m)=(H_{ij}^{\alpha\beta})^{(0)}+\Delta_{ij}^{\alpha\beta}(1,2)[\,&P_1(i\alpha,j\beta)H_{ij}^{\alpha\beta}(m)P_2(i\alpha,j\beta)H_{ij}^{\alpha\beta}(m)P_1(i\alpha,j\beta)\\&-P_2(i\alpha,j\beta)H_{ij}^{\alpha\beta}(m)P_1(i\alpha,j\beta)H_{ij}^{\alpha\beta}(m)P_2(i\alpha,j\beta)] \ .\end{aligned} \tag{B20}$$

We finally insert the explicit expressions (B3) and (B4) for the projection operators $P_r(i\alpha,j\beta)$ and perform at the end according to (B2) the summations over all indices $i,j,\alpha,\beta$. After tedious, but straightforward, manipulations, we arrive at the expression (2.23) for $H_{3d}+H_{3d}^{(U)}=\sum_m H_U(m)$.

---

*Permanent address: Departamento de Física Teórica, Universidad de Valladolid, E-47011 Valladolid, Spain.

[1]J. H. de Boer and E. J. W. Verwey, Proc. Phys. Soc. London **49**, 59 (1937).
[2]B. Brandow, Adv. Phys. **26**, 651 (1977).
[3]B. Brandow (unpublished).
[4]S. Hüfner, J. Osterwalder, T. Riesterer, and F. Hulliger, Solid State Commun. **52**, 793 (1984).
[5]S. Hüfner, P. Steiner, and I. Sander, Solid State Commun. **72**, 359 (1989).
[6]T. M. Wilson, Int. J. Quantum Chem. Symp. **2**, 269 (1968); **3**, 757 (1970).
[7]K. Terakura, T. Oguchi, A. R. Williams, and J. Kübler, Phys. Rev. B **30**, 4734 (1984).
[8]W. Nolting and W. Borgiel, Phys. Rev. B **39**, 6962 (1989).
[9]S. Bei der Kellen, W. Nolting, and G. Borstel, Phys. Rev. B **42**, 447 (1990).
[10]P. W. Anderson, Solid State Phys. **14**, 99 (1963).
[11]V. E. Henrich, Rep. Prog. Phys. **48**, 1481 (1985).
[12]G. A. Sawatzky and J. W. Allen, Phys. Rev. Lett. **53**, 2339 (1984).
[13]P. Kuiper, G. Kruinzinga, J. Ghijsen, G. A. Sawatzky, and H. Verwey, Phys. Rev. Lett. **62**, 221 (1989).
[14]A. Fujimori, F. Minami, and S. Sugano, Phys. Rev. B **29**, 5225 (1984).
[15]A. Fujimori and F. Minami, Phys. Rev. B **30**, 957 (1984).
[16]S. P. Kowalczyk, L. Ley, R. A. Pollack, and D. Shirley, Fig. 13 in Ref. 2.
[17]J. Zaanen, G. A. Sawatzky, and J. W. Allen, Phys. Rev. Lett. **55**, 418 (1985).
[18]M. R. Norman and A. J. Freeman, Phys. Rev. B **33**, 8896 (1986).
[19]G. J. M. Janssen and W. C. Nieuwpoort, Phys. Rev. B **38**, 3449 (1988).
[20]J. P. Perdew and A. Zunger, Phys. Rev. B **23**, 5048 (1981).
[21]A. Svane and O. Gunnarsson, Phys. Rev. Lett. **65**, 1148 (1990).
[22]V. I. Anisimov, M. A. Korotin, and E. Z. Kurmaev, J. Phys.: Condens. Matter **2**, 3973 (1990).
[23]W. Nolting, W. Borgiel, and G. Borstel, Phys. Rev. B **37**, 7663 (1988).
[24]W. Nolting, W. Borgiel, V. Dose, and Th. Fauster, Phys. Rev. B **40**, 5015 (1989).
[25]W. Borgiel and W. Nolting, Z. Phys. B **78**, 241 (1990).
[26]J. Hubbard, Proc. R. Soc. London, Ser. A **276**, 238 (1963).
[27]G. Geipel and W. Nolting, Phys. Rev. B **38**, 2608 (1988).
[28]K. A. Chao, J. Spalek, and A. M. Oleś, J. Phys. C **10**, L271 (1977).
[29]P. W. Anderson, Science **235**, 1196 (1987).
[30]J. Kanamori, Prog. Theor. Phys. **30**, 275 (1963).
[31]D. N. Zubarev, Fortschr. Phys. **9**, 275 (1961).

[32]W. Nolting, *Quantentheorie des Magnetismus* (Teubner-Verlag, Stuttgart, 1986), Vol. 2, p. 157.
[33]R. J. Lad and V. E. Henrich, Phys. Rev. B **38**, 10 860 (1988).
[34]J. M. McKay and V. E. Henrich, Phys. Rev. Lett. **53**, 2343 (1984).
[35]K. S. Kim, Phys. Rev. B **11**, 2177 (1975).
[36]D. E. Eastman and J. L. Freeouf, Phys. Rev. Lett. **34**, 395 (1975).
[37]S. P. Kowalczyk, L. Ley, R. A. Pollack, and D. Shirley, see Fig. 15 in Ref. 2.
[38]A. Fujimori, N. Kimizuka, M. Tanigushi, and S. Suga, Phys. Rev. B **36**, 6691 (1987).
[39]J. Kübler and A. R. Williams, J. Magn. Magn. Mater. **54-57**, 603 (1986).
[40]H. A. Alperin, J. Phys. Soc. Jpn. Suppl. B **17**, 12 (1962).
[41]B. E. F. Fender, A. J. Jacobson, and F. A. Wegwood, J. Chem. Phys. **48**, 990 (1968).
[42]A. K. Cheetham and D. A. O. Hope, Phys. Rev. B **27**, 6964 (1983).
[43]S. Hüfner, Z. Phys. B **58**, 1 (1984).